

**INVESTIGATION INTO SINGLE PIXEL IMAGING:
IMAGES WITHOUT A CAMERA**

AU ZHISHAN

**A project report submitted in partial fulfilment of the
requirements for the award of Bachelor of Engineering
(Honours) Mechatronics Engineering**

**Lee Kong Chian Faculty of Engineering and Science
Universiti Tunku Abdul Rahman**

April 2020

DECLARATION

I hereby declare that this project report is based on my original work except for citations and quotations which have been duly acknowledged. I also declare that it has not been previously and concurrently submitted for any other degree or award at UTAR or other institutions.

Signature :



Name : Au Zhishan


ID No. : 1503203

Date : 21/4/2020

APPROVAL FOR SUBMISSION

I certify that this project report entitled “**INVESTIGATION INTO SINGLE PIXEL IMAGING: IMAGES WITHOUT A CAMERA**” was prepared by **Au Zhishan** has met the required standard for submission in partial fulfilment of the requirements for the award of Bachelor of Engineering (Honours) Mechatronics Engineering at Universiti Tunku Abdul Rahman.

Approved by,

Signature : 
Department of Electrical and Electronic Engineering
Lee Kong Chian Faculty of Engineering and Science
Universiti Tunku Abdul Rahman

Supervisor : Chua Sing Yee

Date : 23/4/2020

Signature : 

Co-Supervisor : Chai Tong Yuen

Date : 23/4/2020

The copyright of this report belongs to the author under the terms of the Copyright Act 1987 as qualified by the Intellectual Property Policy of Universiti Tunku Abdul Rahman. Due acknowledgment shall always be made of the use of any material contained in, or derived from, this report.

© 2019, Au Zhishan. All right reserved.

ACKNOWLEDGEMENTS

I would like to thank everyone who had contributed to the successful completion of this project. I would like to express my gratitude to my research supervisor, Dr. Chua Sing Yee for her invaluable advice, guidance and her enormous patience throughout the development of the research.

In addition, I would also like to express my gratitude to my loving parents and friends who had helped and given me encouragement throughout my university life.

ABSTRACT

Over the past decades, CCD and CMOS have been dominating in the imaging sensor technology. Due to the cost and technological constraints especially in the unusual wavelengths and low light condition, single pixel imaging becomes an important alternative. This approach samples the target scene with a set of micro-structured light masks and obtain the spatial information using only a simple photodiode as the detector. Single pixel imaging strongly depends on the correlation of the mask patterns with the target scene. In this research, various types of mask patterns were studied on their behaviours when sampled with different images. This project conducts a simulation study on single pixel imaging, analyses various mask patterns and reviews their results to form a conclusion.

Masks can be separated into 2 categories, Deterministic (Fourier and Hadamard) and Pseudo-random (Random and Gaussian) masks. As summarized from the results, Random mask has the shortest masking time while Hadamard Mask shows the shortest image reconstruction time. In general, Pseudo-random masks are better for images with random details throughout the images, meanwhile Deterministic masks outperform for simple images. However, Deterministic masks can be customized to give better performance at sampling certain random images. Furthermore, Deterministic masks can be pre-loaded and the imaging results are 100% reproducible while it's not possible for Pseudo-random masks.

In conclusion, Deterministic masks are overall preferred as compared to Pseudo-random masks. This in-depth investigation establishes a comprehensive understanding of the mask patterns and their influence on the performance of single pixel imaging.

TABLE OF CONTENTS

DECLARATION	1
APPROVAL FOR SUBMISSION	2
ACKNOWLEDGEMENTS	4
ABSTRACT	5
TABLE OF CONTENTS	6
LIST OF TABLES	8
LIST OF FIGURES	10

CHAPTER

1	INTRODUCTION	12
	1.1 General Introduction	12
	1.2 Problem Statement	13
	1.3 Aims and Objectives	14
	1.4 Scope and Limitation of the Study	15
	1.5 Contribution of the Study	15
	1.6 Outline of Report	15
2	LITERATURE REVIEW	17
	2.1 Introduction	17
	2.2 CCD and CMOS	17
	2.3 Single Pixel Imaging	18
	2.4 Compressive Sensing	20
	2.5 Light Modulation Patterns	24
	2.6 Hadamard Basis	25
	2.7 Uniform Distribution (Random)	27
	2.8 Normal Distribution (Gaussian)	28
	2.9 Fourier Transform	29

2.10	Root Mean Square Error (RMSE)	30
2.11	Peak Signal-to-Noise Ratio (PSNR)	31
2.12	Structural Similarity Index (SSIM)	32
3	METHODOLOGY AND WORK PLAN	34
3.1	Introduction	34
3.2	Research Methodology	34
3.2.1	Light Modulation Patterns (Masks)	34
3.2.2	Test Images	35
3.3	Simulation and Data Analysis	37
3.4	Work Breakdown Structure	38
3.5	Project Plan & Gantt Chart	39
4	RESEARCH RESULTS	41
4.1	Introduction	41
4.2	Results and Discussions	41
4.2.1	Binary Circles (Figure 3.1)	41
4.2.2	Cameraman (Figure 3.2)	43
4.2.3	Phone (Figure 3.3)	45
4.2.4	Flames (Figure 3.4)	47
4.2.5	Rice (Figure 3.5)	48
4.2.6	Face (Figure 3.6)	51
4.2.7	FUW chart (Figure 3.7)	52
4.2.8	Hadamard 50% Sampling Error	54
4.3	Summary of Result Analysis	56
5	CONCLUSION AND RECOMMENDATION	59
5.1	Conclusion	59
5.2	Limitations	60
5.3	Recommendation for Future Research	60
	REFERENCES	61

LIST OF TABLES

Table 2.1:	Differences between CCD & CMOS against Single Pixel Imaging	20
Table 2.2:	Comparison of Pseudo-random Masks vs. Deterministic Masks	27
Table 3.1:	Different type of sampling methods in their respective category	34
Table 4.1 :	Circles 90% sampling ratio	41
Table 4.2 :	Circles 80% sampling ratio	41
Table 4.3 :	Circles 70% sampling ratio	41
Table 4.4 :	Circles 60% sampling ratio	42
Table 4.5 :	Circles 50% sampling ratio	42
Table 4.6 :	Cameraman 90% sampling ratio	43
Table 4.7 :	Cameraman 80% sampling ratio	43
Table 4.8 :	Cameraman 70% sampling ratio	43
Table 4.9 :	Cameraman 60% sampling ratio	43
Table 4.10 :	Cameraman 50% sampling ratio	44
Table 4.11 :	Phone 90% sampling ratio	45
Table 4.12 :	Phone 80% sampling ratio	45
Table 4.13 :	Phone 70% sampling ratio	45
Table 4.14 :	Phone 60% sampling ratio	45
Table 4.15 :	Phone 50% sampling ratio	45
Table 4.16 :	Flames 90% sampling ratio	47
Table 4.17 :	Flames 80% sampling ratio	47
Table 4.18 :	Flames 70% sampling ratio	47
Table 4.19 :	Flames 60% sampling ratio	47

Table 4.20 :	Flames 50% sampling ratio	47
Table 4.21 :	Rice 90% sampling ratio	49
Table 4.22 :	Rice 80% sampling ratio	49
Table 4.23 :	Rice 70% sampling ratio	49
Table 4.24 :	Rice 60% sampling ratio	49
Table 4.25 :	Rice 50% sampling ratio	49
Table 4.26 :	Face 90% sampling ratio	51
Table 4.27 :	Face 80% sampling ratio	51
Table 4.28 :	Face 70% sampling ratio	51
Table 4.29 :	Face 60% sampling ratio	51
Table 4.30 :	Face 50% sampling ratio	52
Table 4.31 :	FUW chart 90% sampling ratio	52
Table 4.32 :	FUW chart 80% sampling ratio	53
Table 4.33 :	FUW chart 70% sampling ratio	53
Table 4.34 :	FUW chart 60% sampling ratio	53
Table 4.35 :	FUW chart 50% sampling ratio	53
Table 4.36 :	Advantages vs Disadvantages of Pseudo-random Masks	58
Table 4.37 :	Advantages vs Disadvantages of Deterministic Masks	58

LIST OF FIGURES

Figure 1.1:	Classification of masks into different groups (Augustin <i>et al.</i> , 2018)	13
Figure 1.2:	Research Approach	15
Figure 2.1:	An array of pixels with a single black pixel	17
Figure 2.2:	Conventional Image Stock Photo	18
Figure 2.3:	Example of dynamic resolution	19
Figure 2.4:	Visual representation of compressive sensing equation in matrix form	21
Figure 2.5:	2-D analogy of ℓ_2 and ℓ_1 of a compressed sensing signal	22
Figure 2.6:	(a)The original sparse signal (b)The signal itself with periodic sampling in red dots and pseudo-random sampling in blue dots (c) Results of periodic sampling (d) Results of pseudo-random sampling.	23
Figure 2.7:	Illustrative example of how a mask works to sense a sparse signal	24
Figure 2.8:	Examples of different 4x4 Hadamard Masks	26
Figure 2.9:	Probability function of uniform distribution (Al-Kheer and Al-Kareem, 2010)	27
Figure 2.10:	Example of normal distribution (Pierce, 2019)	28
Figure 2.11:	DCT matrix function	29
Figure 2.12:	Example of DCT on an image section	30
Figure 3.1:	Black and White Circles	35
Figure 3.2 :	Grayscale Cameraman	35
Figure 3.3 :	Phones	35
Figure 3.4 :	Flames	36
Figure 3.5:	Rice	36

Figure 3.6 :	Face	36
Figure 3.7:	FUW chart	37
Figure 3.8:	Logo of MATLAB	37
Figure 3.9:	Work Breakdown Structure of this project	38
Figure 4.1 :	Best reconstructed image for binary circles (Hadamard 90%)	42
Figure 4.2 :	Best reconstructed image for Cameraman (Fourier 90%)	44
Figure 4.3 :	Best reconstructed image for Phone (Fourier 90%)	46
Figure 4.4 :	Best reconstructed image for Flames (Random 90%)	48
Figure 4.5 :	Best reconstructed image for Rice (Random 90%)	50
Figure 4.6 :	Best reconstructed image for Face (Random 90%)	52
Figure 4.7 :	Best reconstructed image for FUW chart (Fourier 90%)	54
Figure 4.8 :	Binary Circles 50% Hadamard Mask Sampling Error	54
Figure 4.9 :	Grayscale Cameraman 50% Hadamard Mask Sampling Error	55
Figure 4.10 :	Phones 50% Hadamard Mask Sampling Error	55
Figure 4.11 :	Flames 50% Hadamard Mask Sampling Error	55
Figure 4.12 :	Rice 50% Hadamard Mask Sampling Error	55
Figure 4.13 :	Face 50% Hadamard Mask Sampling Error	55
Figure 4.14 :	FUW Chart 50% Hadamard Mask Sampling Error	56
Figure 4.15:	Visual example of how a mask conforms to an image	57

CHAPTER 1

INTRODUCTION

1.1 General Introduction

Single Pixel Imaging is a developing method of obtaining images through devices that are only equipped with a single pixel detector (Rousset *et al.*, 2017). Single pixel imaging is very different from the existing conventional imaging methods that use matrix detectors with a spatial resolution that captures the whole image with an array of pixels, usually ranging in the millions. These conventional methods, i.e., charge-coupled devices (CCD) and complementary metal-oxide semiconductors (CMOS) are cheap due to the availability of mass production for these devices. However, when an imaging system is needed in the range out of the usual visible spectrum, i.e. infrared imaging, the price of using CCD and CMOS usually will skyrocket to 100-1000 times its original amount (Aksenov and Sych, 2018).

So how does single pixel imaging works? By using a quick pixel detector with a Digital Micromirror Array Device (DMD) to project modulating patterns, ‘masks’ onto the object. The single pixel detector then captures the sampling measurements and image is recovered by using compressive sensing based reconstruction algorithms (Mitra, Cossairt and Veeraraghavan, 2014).

One of the most important aspects of single pixel imaging is the ‘mask’, the modulation light pattern that is projected onto the object by the DMD. This is important to single pixel imaging as a mask is needed to sample the image. With the mask, the single pixel detector can use compressive sensing algorithms to sample the image and reconstruct it quickly.

Compressive sensing is an area of study that was first discovered by Emmanuel Candes, Terrence Tao, Justin Romberg, and David Donoho. They changed how sampling is done forever by proving that you can sample a signal even if you do not follow the Shannon-Nyquist Theorem that states that you need to sample the signal at 2 times the frequency to collect sufficient data. Compressed sensing allows for you to sample the data up to 20 times less than the Shannon-Nyquist and still maintain the clarity of the image clearly (Brown and Grice, 2011).

1.2 Problem Statement

Background of Problem

The most important aspect of single pixel imaging is the sampling method used. The mask determines the sampling method and this greatly affects the final image produced. Several masks are currently available and produce satisfying results, such as the Gaussian mask, Hadamard mask, Bernoulli's mask, etc. However, different masks do produce different results.. Therefore, this project would like to investigate the behaviors of various mask types and their influence on single pixel imaging.

Problem statement 1

Lack of In-depth investigation into different Light Modulation Patterns (masks).

In the current research regarding single pixel imaging, there is a clear differentiation of mask. Masks are differentiated into two groups, Deterministic and Pseudo-Random. These groups are further divided into another two groups, stating masks in these categories are either binary or grayscale (Augustin *et al.*, 2018).

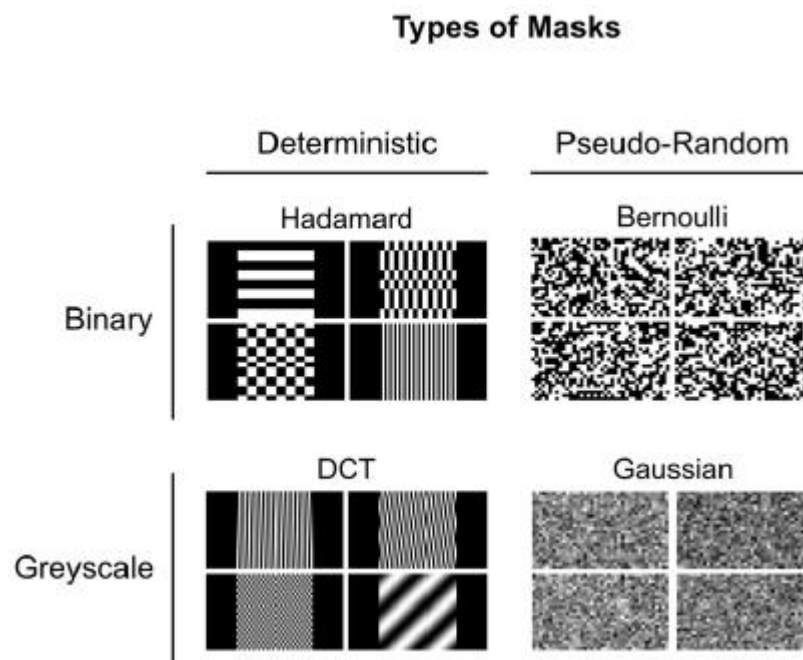


Figure 1.1: Classification of masks into different groups (Augustin *et al.*, 2018)

However, to my knowledge, there aren't any further in-depth studies that investigate the behavior of these masks. For example, if the implementation of a single pixel camera is needed to detect words in pictures, there isn't a simple rubric that allows

for the quick selection of masks for that. Testing out every single mask is needed to determine which is best suited for their objectives and this is a waste of time. Thus, this study is to investigate the behavior of different categories of masks and to show their characteristic.

Problem Statement 2

Deciding the Type of Masks for Different Application

There are many different applications for single pixel imaging out there, ranging from telescopic application (Yu *et al.*, 2014) to MRI scanning (Lustig, Donoho and Pauly, 2007). Which type of masks is better for their respective applications? This is something that this research aims to answer.

Many types of application can benefit from single pixel imaging. For example, Real-time applications require speedy results when taking an image of the object, thus the time taken when reconstructing an image in single pixel imaging will be of utmost importance. Whereas for off-line applications, where urgency isn't needed, it allows for more leeway in regards to time spent on reconstructing the image and places more importance on the quality of the image instead. If, for example, the general time taken for different categories of masks are known, it would allow us to determine which type is better for different application

1.3 Aims and Objectives

This research aims to explore and analyze single pixel imaging as an alternative to conventional imaging techniques. The objectives of this research are:

1. To conduct a simulation study on single pixel imaging. This would eliminate the influence of external factors and produces an ideal case result. This can be a guideline for the real-world application by striving to achieve the simulated results.
2. To analyze light modulation and sampling methods used in single pixel imaging. Different types of light modulation can be explored, be it the ordering of masks or the number of resolutions. Besides, different sampling methods such as Random, Gaussian, Fourier, Hadamard Basis, etc. are studied.
3. To analyze the performance of single pixel imaging. The image reconstructed from the compressive sensing algorithm is evaluated for the effectiveness of the mask used together with masking and reconstruction time. This provides a

comprehensive analysis to show the influence of the masks on the performance of single pixel imaging in terms of image quality, masking, and reconstruction time.

1.4 Scope and Limitation of the Study

This research focuses on the investigation of single pixel imaging based on the problem statement formed. In-depth data analysis was performed based on the findings made.

There is a limitation to this study whereby this study only covers a limited sample size due to the time constraints. Thus, the behaviour of masks was analysed based on the limited types of light modulation and sampling methods but in numbers that are adequate for this study. The results were finalized and concluded after in-depth data collection and analysis.

1.5 Contribution of the Study

This study contributes to furthering the field of single pixel imaging. The finding established allows for the ease of selecting light modulation and sampling methods when setting up single pixel imaging systems for different objectives.

1.6 Outline of Report

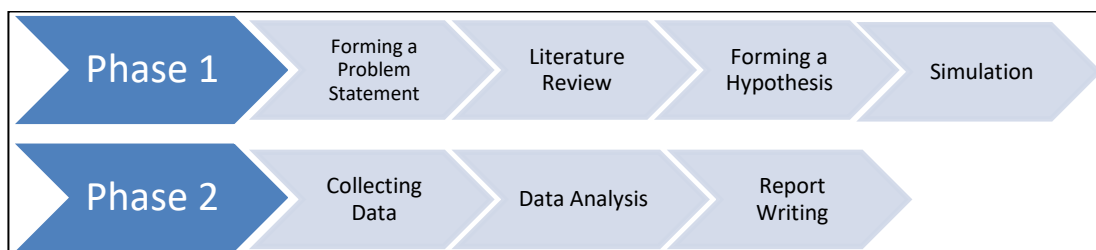


Figure 1.2: Research Approach

The report begins with forming and confirming a specific problem statement. The problem found is the lack of in-depth investigation of light modulation masks and their behaviour. Once the problem is framed, an extensive literature review was written. Areas regarding compressive sensing, light modulation patterns, orders of patterns, etc. are studied and compared thoroughly in the literature review. After that,

a hypothesis is formed, based on the problem statement and the findings in this study's literature review.

Once a hypothesis is formed, the simulation is conducted to confirm this hypothesis. Simulation is to serve as our ideal case result, without any interference from external factors practically. As the simulation is done, data is collected and compared to our hypothesis. Analysis and interpretation of those data are done. Tabulated conclusions are done to represent and convey those data easily. At the very last step, a final report is written to convey what has been done and achieved.

CHAPTER 2

LITERATURE REVIEW

2.1 Introduction

The current imaging industry has developed immensely over the past decade or so ever since the introduction of Charge-Coupled Device (CCD) and Complementary Metal-Oxide-Semiconductor (CMOS). Ever since humans discovered that silicon allows for the conversion of photons at visible wavelengths to an electrical signal, conventional cameras for everyday use had been affordable and accessible. However, the prices of imaging equipment needed to capture images outside the visible wavelength such as medium or far infrared wavelengths are astronomical. Cameras of such calibre are also heavy, bulky and complicated to operate. This is due to the limitation of conventional silicon unable to detect and convert weaker wavelengths of light.

A solution to this is to utilize single pixel imaging. Single pixel imaging utilizes only one single pixel in the image capturing device. This chapter will be comparing conventional imaging methods to single pixel imaging, compressive sensing algorithm and light modulation uses in single pixel imaging.

2.2 CCD and CMOS

Charge-Coupled Device (CCD) and Complementary Metal-Oxide-Semiconductor (CMOS) are conventional image capturing methods that are used in many devices nowadays. They consist of thousands and millions of tiny pixels capturing cells that will capture light from the image and capture them as an array.

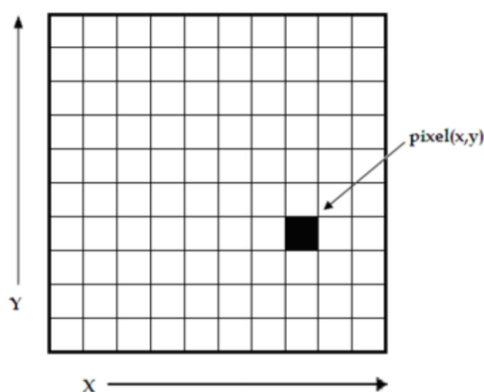


Figure 2.1: An array of pixels with a single black pixel

2.3 Single Pixel Imaging

Different from conventional CCD and CMOS that captures images with a pixel array that consists of thousands to millions of pixels (Taylor, 1998), single pixel imaging detects images with a single pixel and reconstructs them into a picture. This allows for the cost of making a single pixel camera for infrared detection much cheaper as it is just a single pixel, as compared to millions of pixels in CCD and CMOS. Not only that it is cheaper, but single pixel imaging also provides many advantages such as improved detection efficiency, faster response, and resolution flexibility.

One of single pixel imaging strong points is range detection. In a 2014 scientific paper report, a single pixel detector managed to detect a Chinese character on a billboard 2.6km away with a 20cm resolution (Yu *et al.*, 2014). This opens up a whole new area to explore that involves the telescopic industry. Militaries would be able to make cheaper cost detection camera; astronomers would be able to improve their telescope and produce it at a cheaper price and more.

A unique advantage that single pixel imaging methods have is resolution flexibility. In conventional imaging methods, the resolution of a picture is often fixed. Even if the object in question is focused on and the background of the object is blurred, the resolution of the whole picture is still the same.



Figure 2.2: Conventional Image Stock Photo

As shown above, in figure 2.2, an object is focused clearly with the background blurred. However, the resolution of the throughout the image is still the same, 700x467.

There are moments where this isn't ideal, as it takes up more computational power to process the whole image even though only the object in focus is only required. The blurred background will be consuming computation power thus more time will be spent on processing the image as a whole. In single pixel imaging, adaptive imaging methods with dynamic resolution can be achieved. To give an example, an image can have a different resolution in different parts to ease the computational load and reduced the procession time.

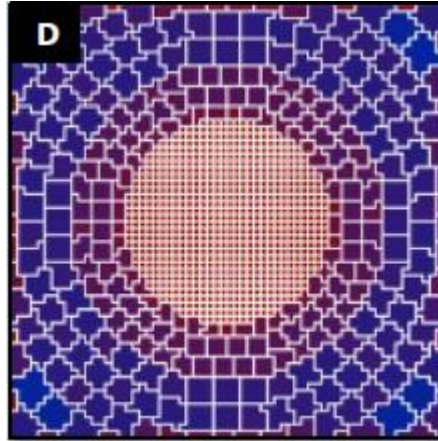


Figure 2.3: Example of dynamic resolution

The above figure is taken from (Barnett *et al.*, 2017), it shows that the dynamic resolution image can be achieved to certain parts of the image. This unique advantage of single pixel imaging allows for faster processing speed and improved detection capabilities, allowing single pixel imaging methods to perform better than conventional imaging methods in places such as face detection. Face detection is used on many occasions, most commonly in our phones. With this method of single pixel imaging, the face could be focused on higher resolution and the background in a lower resolution. This allows for faster processing of the face in question and will unlock our phones much faster.

Unfortunately, there is a disadvantage to single pixel imaging when compared to CMOS and CCD. The largest disadvantage currently in single pixel imaging is the lack of colour in images taken with single pixel imaging methods. This greatly restricts the uses of single pixel imaging in the current world. However, there is still plenty of room for improvement as conventional imaging method used to be restricted in only black and white in just a couple of decades ago. Other than this, there is also a problem with minimizing the size of single pixel imaging equipment. As there is a need for a

DMD to project light modulation patterns, reduction of size is still an issue to be solved for it to be fitted in everyday devices such as mobile phones. Overall, single pixel imaging has plenty of room for improvement and a huge potential to overtake conventional imaging method such as CCD or CMOS in the future.

Table 2.1: Differences between CCD & CMOS against Single Pixel Imaging

CCD & CMOS	Single Pixel Imaging
Captures images with a pixel array (Taylor, 1998)	Captures images pixel by pixel & reconstructs the image (Rousset <i>et al.</i> , 2017)
Expensive equipment needed when taking unconventional images (Aksenov and Sych, 2018)	Cheap equipment when taking unconventional images (Aksenov and Sych, 2018)
Low Visibility when capturing images far away (Yu <i>et al.</i> , 2014)	Clear Visibility even when capturing images far away (Yu <i>et al.</i> , 2014)
Fixed Resolution (Barnett <i>et al.</i> , 2017)	Dynamic Resolution (Barnett <i>et al.</i> , 2017)
Images taken are processed slower (Barnett <i>et al.</i> , 2017)	Images taken can be processed faster (Barnett <i>et al.</i> , 2017)
Captures Colourized images	Captures Grayscale images
Bulky	Compact

2.4 Compressive Sensing

One of the main components that make single pixel imaging works is the algorithm that samples and collects data from the object to reconstruct the final image. Different from conventional imaging methods that use a pixel array to capture the object, single pixel imaging detects and samples the object one pixel at a time and reconstructs them. Thus, the algorithm to sample and reconstruct the image is crucial to the whole operation.

There are many different types of signal sampling method, with the most famous being the Nyquist-Shannon Sampling Theorem. According to Shannon's paper, "If a function $f(t)$ contains no frequencies higher than W cps, it is completely determined by giving its ordinates at a series of points spaced $1/2$ seconds apart."

(Shannon, 1998). Therefore, this theorem states that a sufficient sampling rate of a signal is $2W$ samples per second. This is a problem for single pixel imaging if the Nyquist-Shannon Sampling Theorem is used, as it takes an enormous amount of time to sample at the rate of 2 times the highest frequency in the image. Also, reconstructing the image would take a huge amount of time as well. Single pixel imaging would be an inefficient, arduous and wasteful process if the Nyquist-Shannon theorem was used.

Fortunately, there is another sampling theorem out there that is perfect for single pixel imaging; Compressive Sensing. The general theory of Compressive Sensing was discovered by Emmanuel Candes, Justin Romberg and Terence Tao in a 2006 paper regarding Stable Signal Recovery from incomplete and inaccurate measurements. They state that,

$$y = Ax_0 \quad (2.1)$$

where

$x_0 \in \mathbb{R}^n$ = represents the original signal or image

A = sensing matrix n by m with rows fewer than columns

y = Sampled signal

and it is possible to recover the signal x_0 accurately based on sample y (Candès, Romberg and Tao, 2006).

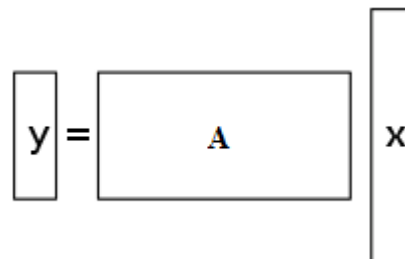


Figure 2.4: Visual representation of compressive sensing equation in matrix form

A compressive sensing algorithm works on sparse signals, which means that signals that are not already compressed. For compressed signals, sampling of these signal still follows the Nyquist-Shannon's theorem. However, most natural signals around us are sparse and that includes images. Therefore, compressive sensing allows single pixel imaging to sample at a rate much lower than the Nyquist-Shannon theorem and will allow us to reconstruct the data back accurately. In a paper regarding

compressive sensing and its uses in MRI by (Lustig, Donoho and Pauly, 2007), they compared the angiogram of the arteries in a human leg by using both Nyquist-Shannon and Compressed Sensing sampling method. When the sampling rate goes lower and lower until 20-fold the under-sampling rate, the Nyquist-Shannon reconstructed images were degraded lower and lower. However, the angiogram with compressed sensing sampling was still crisp and clear even at 20-fold under-sampling. This shows that compressed sensing allows for faster and shorter sampling time and yet still manage to reconstruct the image back accurately, which is ideal for single pixel imaging that requires fast and precise image reconstruction.

Reconstructing of signal in compressed sensing is based heavily on the ℓ_1 - norm, as we know that y that was sampled from the whole image is from a high sparse signal, thus a sensible decoding method is to look for the sparsest signal among those to produce a computationally traceable linear program (Zhang, 2013):

$$\min \{ \|x\|_1 : y = Ax \}$$

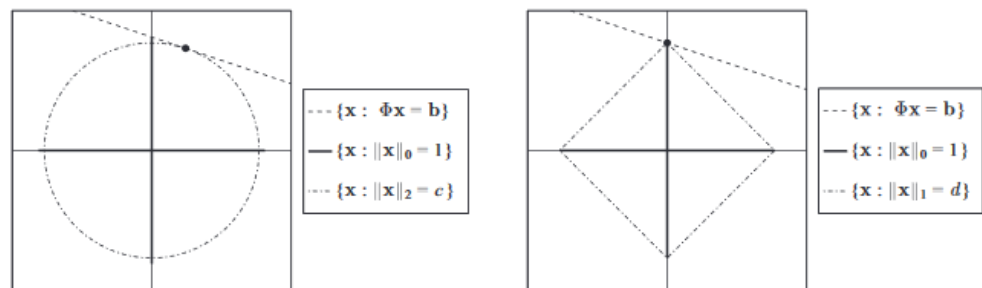


Figure 2.5: 2-D analogy of ℓ_2 and ℓ_1 of a compressed sensing signal

But why ℓ_1 - norm? Why not ℓ_2 - norm? According to a research paper published by Kurt Bryan and Tanya Leise, by using ℓ_2 - norm, the analog on the left in figure 2.5 will form. This does not promote sparsity as there is an x and y vector where the circle intersects with the line. However, when ℓ_1 - norm is used instead a diamond-like shape is formed and the line is more often than not intersecting the edge of the diamond. This allows for a just a y vector and not an x vector or vice versa, promoting sparsity (Bryan and Leise, 2013).

There are several main ingredients to compressed sensing. First, a signal must be sparse and we talked about that. Second, measurements must be “incoherent”. Lastly, there must be sufficiently many measurements.

For measurements to be “incoherent”, it means that sampling of a signal cannot be periodic and even. This is due to the nature of the sparsity of a signal.

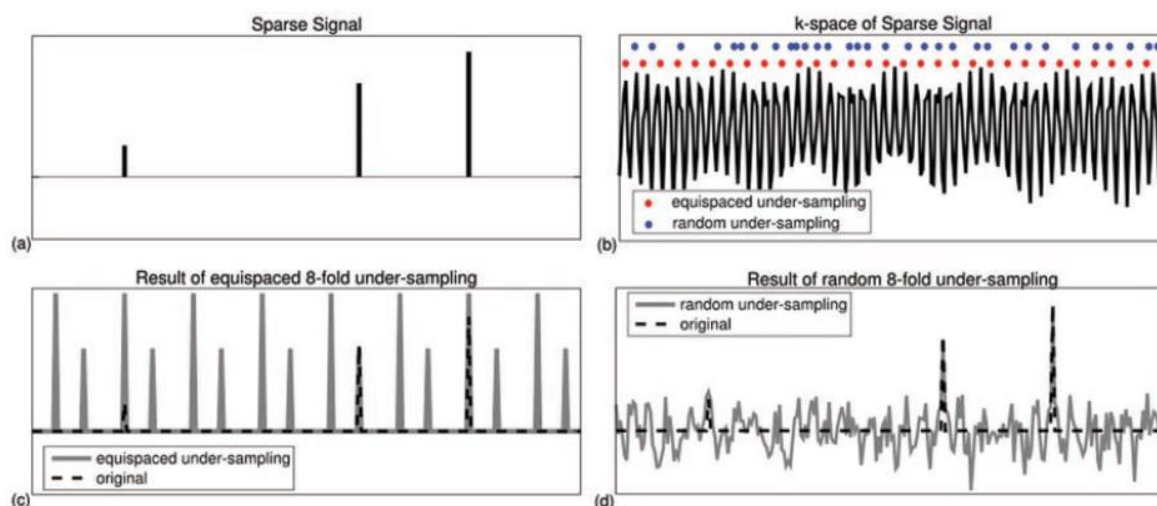


Figure 2.6: (a)The original sparse signal (b)The signal itself with periodic sampling in red dots and pseudo-random sampling in blue dots (c) Results of periodic sampling (d) Results of pseudo-random sampling.

If a signal is measured periodically, a coherent aliasing signal that is produced that cannot be recovered as there is no way to tell apart which spike is genuine or an imposter. However, pseudo-random sampling will allow for the 2 highest spikes to be noticed from the background “noise”. The 3rd spike can be recovered with an iterative threshold procedure (Lustig, Donoho and Pauly, 2007).

So why does compressed sensing works? How does a signal recover itself just from a low number of samples? This is mainly due to the Restricted Isometry Property (RIP), a concept introduced by Emmanuel Candès and Terence Tao. The RIP states that:

$$(1 - \delta_s) \|x\|_2^2 \leq \|Ax\|_2^2 \leq (1 + \delta_s) \|x\|_2^2$$

for all S -sparse vector of x . This states that matrix A is definite to only change the length of any vector x "slightly" as long as the vector x is at least S -sparse (Cand, 2008). This also means that the inner product of sparse vectors is preserved during compressed sensing, this allows us to preserve the core relations of the sparse vectors thus making recovery of the signal possible. Another important aspect that RIP preserves are the correlations of data, this allows for data such as the distances of 2 vectors to be preserved even under compression. Lastly, fast numerical linear algebra

can be done onto compressed data due to RIP and this allows for faster computation for large data.

2.5 Light Modulation Patterns

One of the most important elements in single pixel imaging is the sampling method. The pixel detector is only able to detect the object if there is a mask on the object. In the previous subsection, it is stated that a sensing matrix A is needed in the general equation of compressed sensing. This sensing matrix is the light modulation pattern, also known as “mask” needed. This light modulation pattern is illuminated onto the object with a Digital Micromirror Device (DMD) or a Spatial light modulator (SLM). Many different types of light patterns could be used as a sensing matrix for single pixel imaging. The many different light patterns out there could generally be separate into 2 groups, deterministic patterns or pseudo-random patterns as shown in figure 1.1 (Augustin *et al.*, 2018).

So how does the sensing matrix help the sampling of a non-zero sparse signal? The sensing matrix or light modulation mask consists of random entries of +1 or -1; when the mask is applied onto the image, this sparse signal will be located either on the +1 or -1 entries of the matrix (Nowak, 2006).

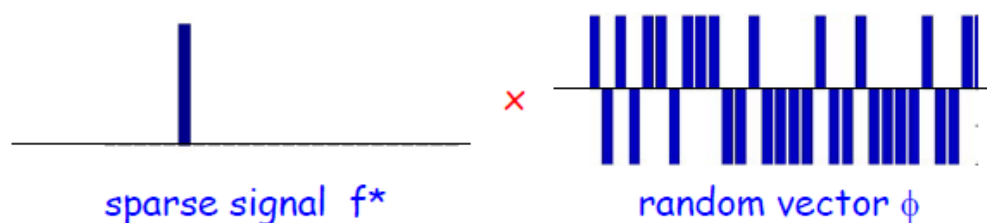


Figure 2.7: Illustrative example of how a mask works to sense a sparse signal

There are many masks out there that can be used as a sensing matrix, a few famous ones are Hadamard Basis and Discrete Cosine Transform (DCT) that falls under the deterministic mask or Bernoulli Transform and Gaussian Transform that falls under the pseudo-random mask’s category. Not all masks are categorized under these two categories, but most are. So how do we know which is better? Deterministic or pseudo-random? Well, there isn’t an answer to which is the better mask as both types are equally good, just at different things. Previously in compressive sensing, figure 2.6, it shows that random sampling is much better than sampling at regular

interval which in a sense is a deterministic sampling. Random sampling mask is supposedly better than a normal deterministic mask since sampling at regular intervals means that some sparse data might be missed. Random sampling will allow for a better chance of collecting the sparse signal in a data set when the number of sampling increases while sampling at regular intervals will not result differently. However, if this is the case, why is the most popular light modulation sampling method in the single pixel imaging industry using Hadamard basis, a deterministic mask?

First, let's discuss random sampling masks. They are usually Gaussian model masks or Bernoulli's transform model masks that mimic randomness. These are simple and fast to generate as there are usually algorithms to generate them. However, as good as these masks are, there are a few downsides to them. When these masks are applied onto a huge object, the reconstruction time of the object is usually very long after the single pixel detects the object. This is because of the incoherent nature of the mask with the spatial properties of the object, such that each measurement provides a tiny amount of information about every pixel (Edgar, Gibson and Padgett, 2019). This will lead to the reconstruction time of the image to be much larger than the acquisition time, which makes it seem like the compressive sensing of the object was useless in the first place. They are also not efficient, requiring lots of storage spaces with no way to recover RIP properties (Nguyen and Shin, 2013). Nevertheless, using a pseudo-random mask for an application that isn't pressed to be done in real-time will still produce a very good quality image.

2.6 Hadamard Basis

This led us to deterministic masks. The deterministic masks single pixel imaging utilizes is different from the conventional regular interval sampling method. One of the most popular deterministic masks used for single pixel imaging is Hadamard Basis mask, Hadamard basis masks is a 2^N square matrix whose values are either +1 or -1 (Hadamard, 1893).

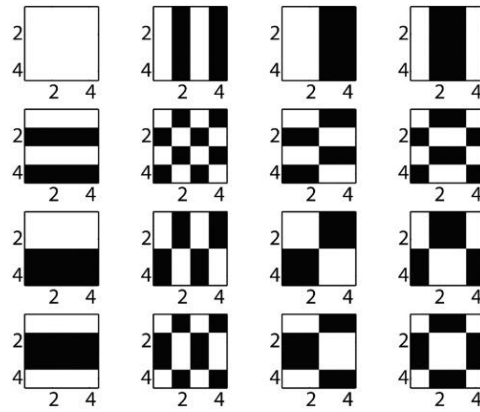


Figure 2.8: Examples of different 4x4 Hadamard Masks

These masks are applied one after another onto the object, this allows the sampling of the image to be deterministic yet not at a regular interval. These masks are not exactly incoherent with the spatial properties of the object, the masks are applied one-by-one onto the object with the single pixel detector taking the resultant light intensity of each mask. After that, a fast reconstruction of the image can be done. For example, it could be as simple as taking the transpose of the Hadamard matrix and getting back the original image of the object, etc. This allows for faster and more efficient reconstruction times of the image yet bypassing the problem of sampling at a regular interval.

A unique advantage to Hadamard Basis masks that most of the other deterministic masks don't have is the many manipulative method in arranging it. An example would be rearranging it in a Russian Doll-like manner. This is an optimized measurement that allows for minimal computational overhead instead of applying the Hadamard Masks randomly which results in faster image processing (Sun *et al.*, 2017). Other than the Russian Doll method, Hadamard Basis mask could also be manipulated in ways such as rearranging it similar to an origami folding model. This allows for better image quality and decreasing the uncertainty of the pattern sequence at the same time, allowing for the reduction of sampling ratio by 0.5% which is important for the realization of real-time compressed sensing single pixel imaging (Yu and Liu, 2019). Lastly, there are also methods to utilize Hadamard Basis masks to manipulate the resulting resolution of the sampled image. By using Hadamard Basis mask with different resolution, e.g. 4x4, 8x8, etc., the image output will be of that resolution. This allows for quicker object detection in various applications as the resolution and details could be redundant in those cases (Zhou *et al.*, 2018).

Table 2.2: Comparison of Pseudo-random Masks vs. Deterministic Masks

Pseudo-random masks	Deterministic Masks
Fast and easy to construct	Slow and tedious to construct
Less efficient (Nguyen and Shin, 2013)	More efficient (Nguyen and Shin, 2013)
Takes up more memory storage (Nguyen and Shin, 2013)	Takes up lesser memory storage (Nguyen and Shin, 2013)
Long image reconstruction time (Sun <i>et al.</i> , 2017)	Shorter image reconstruction time (Sun <i>et al.</i> , 2017)
Less flexibility	More flexibility (Zhou <i>et al.</i> , 2018)
Suited for off-line application	Suited for real-time application (Yu and Liu, 2019)

2.7 Uniform Distribution (Random)

Continuous uniform distribution will consist of a constant probability density within a stated range. The continuous uniform distribution in the range (0, 1) has connections with the probability integral transformation, and with the exponential, logistic, and beta distributions. Some characterizations of functions of two independent random variables are given. (Deng, 2014)

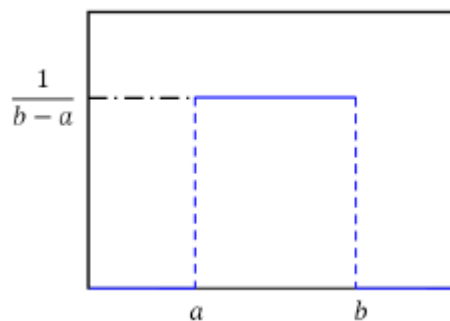


Figure 2.9: Probability function of uniform distribution (Al-Kheer and Al-Kareem, 2010)

$$f(x) = \begin{cases} \frac{1}{b-a} & \text{for } a \leq x \leq b, \\ 0 & \text{for } x < a \text{ or } x > b \end{cases} \quad (2.2)$$

Uniform Distribution states all intervals between **a** and **b** are equally probable, thus ensuring an even chance to get any value between **a** and **b** during the selection of a value.

By using a uniform distribution function in creating a mask for single pixel imaging, this will ensure that the mask is equally distributed with no advantage in detecting any sort of image. This also allows for simple and fast mask construction as the function for creating a uniform distribution mask is easy and short.

2.8 Normal Distribution (Gaussian)

The normal distribution, or also known as Gaussian Transform is a probability distribution that is symmetric around the mean. It shows that data are more likely to occur around the mean rather than away from the mean. As a graph, normal distribution will appear as a bell curve. (Chen, 2019)

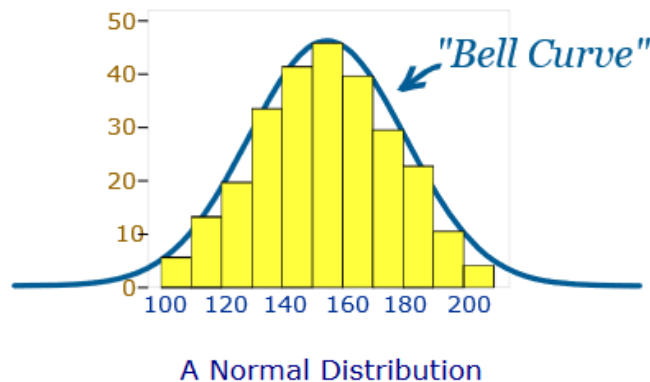


Figure 2.10: Example of normal distribution (Pierce, 2019)

Standard gaussian transform has 2 parameters, the mean and the standard deviation. In a normal distribution, 68% of the data are within +/- 1 standard deviation of the mean, 95% are within +/- 2 standard deviations, and 99.7% are within +/- 3 standard deviations. This shows that most of the time, a majority of the data will converge towards the mean even while randomness is applied.

Applying Gaussian Transform to create a mask for single pixel imaging will affect the image in such a way that the majority of the focus will be at the centre of the image. This will affect the reconstruction of the image such that details at the edge of

the image will be either blurred or missing. Although there are drawbacks to using Gaussian Transform as a mask for single pixel imaging, the advantages are that if the object in question is in the middle of the image, this allows for ease of mask construction as Gaussian Transform function are usually a built-in component in most software libraries.

2.9 Fourier Transform

Fourier Transform is a very important transformation that allows us to convert an image that is in the spatial domain into an equivalent frequency domain. In a Fourier domain image, each point represents a particular frequency contained in the spatial domain image. (R.Fisher *et al.*, 2003)

However, Fourier transform contains complex numbers and has issues with poor energy compaction. Therefore, it is difficult to use it as a mask for single pixel imaging as constructing a mask with complex numbers is time and resource-consuming (Vasconcelos, 2015). However, Discrete Cosine Transform (DCT) has the properties of Fourier Transform but without the complex numbers. As cosine is from -1 to 1, the DCT will only consist of real numbers.

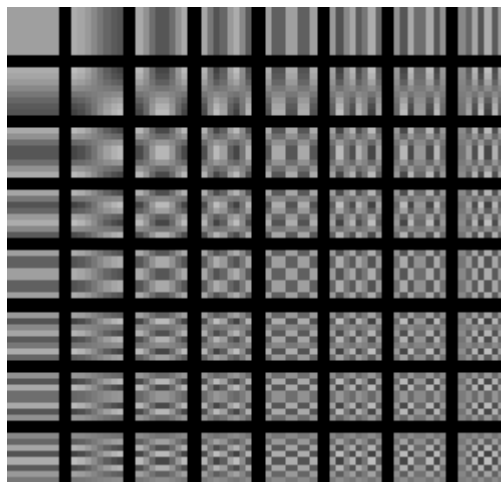


Figure 2.11: DCT matrix function

The above figure shows us the DCT matrix function. This will be the mask that applies to the image in single pixel imaging. The image in question will be weighted in regards to the 8x8 section of the DCT matrix function. This allows us to determine the sparsity of the image as the higher frequency signals in the image can be wiped out due to it being unimportant to the image. Usually, images will be weighted more

towards the top left of the matrix, compared to the higher frequency bottom right matrix. This deterministic method allows for image compression and faster image sampling compared to random sampling such as normal and uniform distribution as those methods will still take those unimportant signals in question. Below is an example of a section of an image that undergoes DCT and has those unimportant signals removed.

$$\begin{bmatrix} -415 & -30 & -61 & 27 & 56 & -20 & -2 & 0 \\ 4 & -22 & -61 & 10 & 13 & -7 & -9 & 5 \\ -47 & 7 & 77 & -25 & -29 & 10 & 5 & -6 \\ -49 & 12 & 34 & -15 & -10 & 6 & 2 & 2 \\ 12 & -7 & -13 & -4 & -2 & 2 & -3 & 3 \\ -8 & 3 & 2 & -6 & -2 & 1 & 4 & 2 \\ -1 & 0 & 0 & -2 & -1 & -3 & 4 & -1 \\ 0 & 0 & -1 & -4 & -1 & 0 & 1 & 2 \end{bmatrix} \xrightarrow{\text{red arrow}} \begin{bmatrix} -26 & -3 & -6 & 2 & 2 & -1 & 0 & 0 \\ 0 & -2 & -4 & 1 & 1 & 0 & 0 & 0 \\ -3 & 1 & 5 & -1 & -1 & 0 & 0 & 0 \\ -4 & 1 & 2 & -1 & 0 & 0 & 0 & 0 \\ 1 & 0 & 0 & 0 & 0 & 0 & 0 & 0 \\ 0 & 0 & 0 & 0 & 0 & 0 & 0 & 0 \\ 0 & 0 & 0 & 0 & 0 & 0 & 0 & 0 \\ 0 & 0 & 0 & 0 & 0 & 0 & 0 & 0 \end{bmatrix}$$

Figure 2.12: Example of DCT on an image section

2.10 Root Mean Square Error (RMSE)

Root Mean Square Error (RMSE) is the measurement of how much error is there between 2 data sets, in our case that would be the original image and the reconstructed image (*How to Calculate Root Mean Square Error (RMSE) in Excel - GIS Geography*, 2014).

$$\text{RMSE} = \sqrt{\frac{\sum_{i=1}^n (P_i - O_i)^2}{n}} \quad (2.3)$$

P represents the Predicted image

O represents the original image

n represents the sample size

As the error between them is squared, the output will always be positive and thus the order does not matter as long it order doesn't change throughout. Also, as the errors are squared, this means that RMSE gives larger weightage towards large errors. This is useful as a large error in image processing is usually undesirable.

RMSE quantifies how different the 2 images are. The smaller the RMSE, the closer the 2 images are to each other.

2.11 Peak Signal-to-Noise Ratio (PSNR)

Peak Signal-to-Noise Ratio (PSNR) is an expression for the ratio between the maximum possible value (power) of a signal and the power of distorting noise that affects the quality of its representation. Because many signals have extensive dynamic ranges, (ratio between the largest and smallest possible values of a changeable quantity) the PSNR is usually expressed in terms of the logarithmic decibel scale (dB) (*Peak Signal-to-Noise Ratio as an Image Quality Metric - National Instruments, 2019*).

$$PSNR = 20 \log_{10} \left(\frac{MAX_f}{\sqrt{MSE}} \right) \quad (2.4)$$

Where MSE (Mean Squared Error) is

$$MSE = \frac{1}{mn} \sum_0^{m-1} \sum_0^{n-1} \|f(i,j) - g(i,j)\|^2 \quad (2.5)$$

f represents the matrix data of our original image

g represents the matrix data of our degraded image in question

m represents the numbers of rows of pixels of the images and i represents the index of that row

n represents the number of columns of pixels of the image and j represents the index of that column

MAX_f is the maximum signal value that exists in our original “known to be good” image

The reason for using PSNR as an image quality metric is that MSE allows us to compare the true pixel values of our original image to our reconstructed image. Thus, the higher the PSNR, the better the quality of the reconstructed image is to the original image and therefore the better the mask used to sample the image. Also, when using 2 identical images to compute the MSE it will be 0 and thus the PSNR will be undefined as it is divided by 0.

2.12 Structural Similarity Index (SSIM)

The simplest and most widely used quality metric is the mean squared error (MSE), computed by averaging the squared intensity differences of distorted and reference image pixels, along with peak signal-to-noise ratio (PSNR). These are appealing because they are simple to calculate, have clear physical meanings, and are mathematically convenient in the context of optimization. However, they are not very well matched to perceived visual quality (Wang *et al.*, 2004). Therefore, the Structural Similarity (SSIM) Index was created. It measures the perceptual *difference* between two similar images. It is unable to judge which of the two is better; to know that, it must be inferred from knowing which is the “original” and which has been subjected to additional processing such as data compression (*SSIM: Structural Similarity Index / imatest*, no date)

$$\begin{aligned}
 l(x, y) &= \frac{2\mu_x\mu_y + c_1}{\mu_x^2 + \mu_y^2 + c_1} \\
 c(x, y) &= \frac{2\sigma_x\sigma_y + c_2}{\sigma_x + \sigma_y + c_2} \\
 s(x, y) &= \frac{\sigma_{xy} + c_3}{\sigma_x\sigma_y + c_3}
 \end{aligned}
 \tag{2.6}$$

The SSIM formula is based on three comparison measurements between the samples of x and y : luminance (l), contrast (c) and structure (s) (Wang, Simoncelli and Bovik, 2003).

With these 3 components, the SSIM can be calculated by

$$\text{SSIM}(x, y) = \frac{(2\mu_x\mu_y + c_1)(2\sigma_{xy} + c_2)}{(\mu_x^2 + \mu_y^2 + c_1)(\sigma_x^2 + \sigma_y^2 + c_2)}
 \tag{2.7}$$

with

μ_x represents the average of x

μ_y represents the average of y

σ_x^2 represents the variance of x

σ_y^2 represents the variance of y

σ_{xy} represents the covariance of x and y

c_1 and c_2 represent 2 variables to stabilize the division with a weak denominator

Using SSIM as a quality metric, we can tell how similar is the reconstructed image to the original image based on our Human Visual System (HVS). For an SSIM value of 1, it means that the two images are perfectly identical, whereas with a value of 0 it means that the two images are completely different. By using this quality metric in our data analysis, we can determine which image output by different mask sample are more similar to the original to the HVS.

CHAPTER 3

METHODOLOGY AND WORK PLAN

3.1 Introduction

This chapter contains the details about how the data is prepared, collected and analysed. Furthermore, a detailed work plan, Work Breakdown Structure (WBS) and Gantt chart were created to manage the project activities and ensure timely completion of the project.

3.2 Research Methodology

3.2.1 Light Modulation Patterns (Masks)

According to the problem statement stated in chapter 1, the analytics of different masks behaviours will be done. First, masks are split into 2 categories: deterministic and pseudo-random (Augustin *et al.*, 2018).

Table 3.1: Different type of sampling methods in their respective category

Deterministic Masks	Pseudo-Random Masks
Hadamard Basis	Uniformly Distributed pseudo-random
Fourier Transform	Gaussian Transform

Next, we will use these masks and test them on various images. These images will be run through simulation as the object that is being captured by a single pixel camera, the images will be sampled with the various masks and the results will be analysed thoroughly. Various behaviour can be analysed based on the number of samples, resolution sized, and many other parameters that can quantify the quality of the image produced.

3.2.2 Test Images

To test the various masks, a set of images have been prepared.

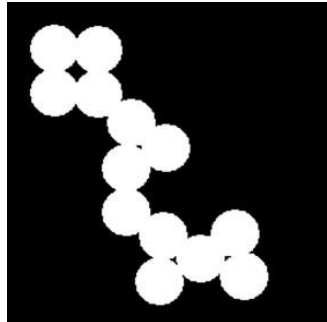


Figure 3.1: Black and White Circles

First, a simple binary image as shown in Figure 3.1. It serves as a baseline for all masks, letting us know which mask is better at sampling a simple binary image.



Figure 3.2 : Grayscale Cameraman

Next up is a grayscale image. Figure 3.2 is a cameraman in grayscale, this allows us to test the performance of the various masks on grayscale images. Also, Figure 3.2 is a humanoid figure, this will test the masks on detecting humanoid images.



Figure 3.3 : Phones

The third is a simple square-ish image. As shown in Figure 3.3, the phones in the image are very simple looking, with details that are not randomly spread out in the image. This allows us to know which masks are better with non-random images.



Figure 3.4 : Flames

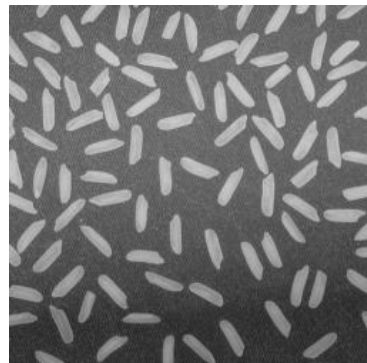


Figure 3.5: Rice

Figure 3.4 and Figure 3.5 allows us to test the masks detection capability on images with random details all around the image.



Figure 3.6 : Face

Figure 3.6 is a human face, which is technically in the same category as Figures 3.4 and 3.5. Every face is different with details random throughout the image.

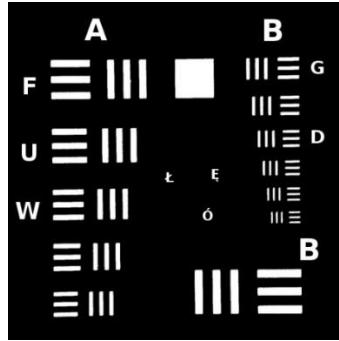


Figure 3.7: FUW chart

Figure 3.7 is an FUW chart. It is a chart that is usually used as a test image for various applications. It is a binary image, with various sizes of stripes in both horizontal and vertical direction, and alphabets in different sizes. As most image testing uses this image, we will be testing this image too as a reference to other studies.

3.3 Simulation and Data Analysis

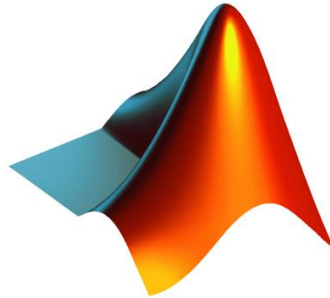


Figure 3.8: Logo of MATLAB

The single pixel imaging process was simulated in MATLAB. A simulation is easier and faster to acquire results on the study of light modulation patterns, as this allows us to eliminate the environmental and external factor due to hardware. MATLAB is chosen for its user-friendly platform and helpful resources that are available on the internet.

Images from Figure 3.1 will be simulated as if it is a picture taken in the real world with a single pixel camera, masks will then be placed over them to simulate an SLM/DMD device projecting the mask onto the object. After that, the sampling process will be simulated. Reconstruction of the image is then done and it will be evaluated with factors such as time is taken, resolution and quality of the image.

The computational time for each image to process through each mask will be recorded and compared. Next, the quality and resolution of the image is also a deciding factor as the captured image needs to be clear and precise to provide valuable information to the user. These two factors will give a clear idea of the different behaviours for different types of masks.

3.4 Work Breakdown Structure

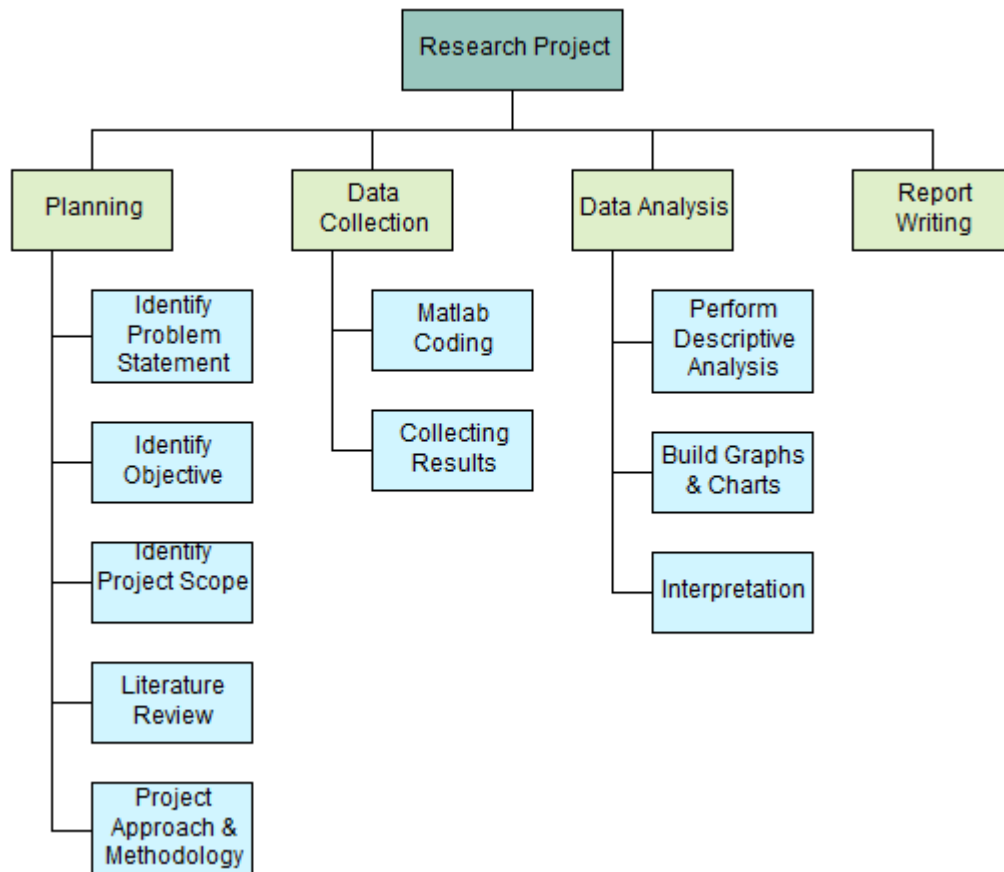
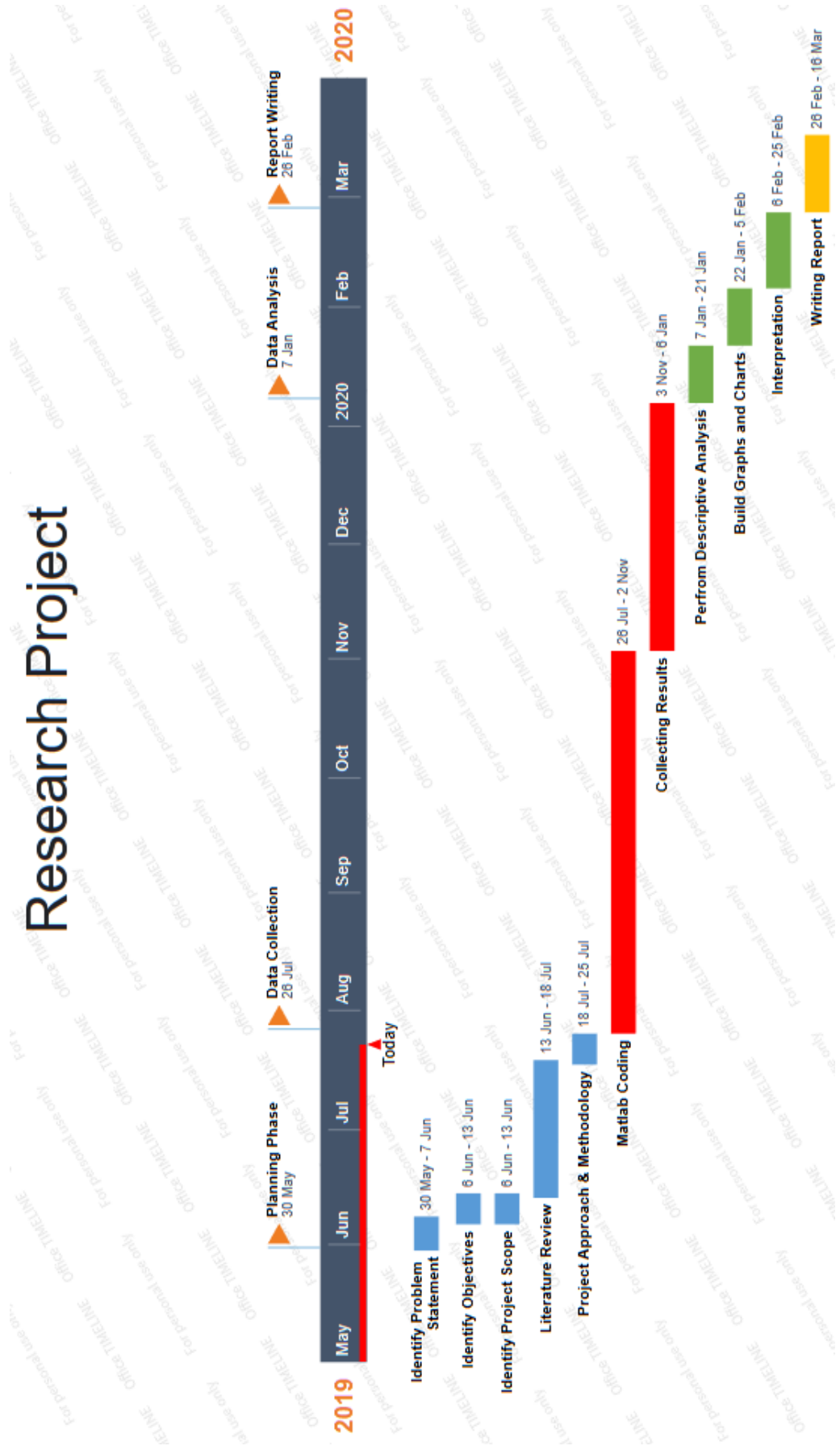


Figure 3.9: Work Breakdown Structure of this project

3.5 Project Plan & Gantt Chart

Task Name	Duration(days)	Start Date	End Date
Planning Phase	41	30 May 2019	25 July 2019
Identify Problem Statement	7	30 May 2019	7 June 2019
Identify Objectives	6	6 June 2019	13 June 2019
Identify Project Scope	8	6 June 2019	13 June 2019
Literature Review	26	13 June 2019	18 July 2019
Project Approach & Methodology	6	18 July 2019	25 July 2019
Data Collection	117	26 July 2019	6 January 2020
Matlab Coding	71	26 July 2019	2 November 2019
Collecting Results	46	3 November 2019	6 January 2020
Data Analysis	36	7 January 2020	25 February 2020
Perform Descriptive Analysis	11	7 January 2020	21 January 2020
Build Graphs and Charts	11	22 January 2020	5 February 2020
Interpretation	14	6 February 2020	25 February 2020
Report Writing	14	26 February 2020	16 March 2020
Writing Report	14	25 February 2020	16 March 2020

Research Project



CHAPTER 4

RESEARCH RESULTS

4.1 Introduction

Chapter 4 outlines the outcome of the research. The research was completed by MATLAB simulation and the data obtained was tabulated using Excel. The results for each test image were analysed and discussed.

4.2 Results and Discussions

4.2.1 Binary Circles (Figure 3.1)

Table 4.1 : Circles 90% sampling ratio

90%	Random	Gaussian	Fourier	Hadamard
RMSE	0.0480	0.0493	0.0249	0.0248
SSIM	0.4226	0.4103	0.6714	0.6906
PSNR	26.3991	26.1305	32.1825	32.1589
end time	92.0475	94.6590	99.5980	109.4191
mask time	4.6746	6.2026	6.0016	5.7147
recon time	86.2920	88.1943	92.5002	103.0032

Table 4.2 : Circles 80% sampling ratio

80%	Random	Gaussian	Fourier	Hadamard
RMSE	0.0641	0.0599	0.0259	0.0343
SSIM	0.3805	0.3901	0.6365	0.5003
PSNR	23.8662	24.4667	31.7963	29.2586
end time	87.5186	91.5957	90.0122	88.8064
mask time	3.5347	5.6811	5.4873	5.1065
recon time	83.7724	85.6446	83.4426	82.9853

Table 4.3 : Circles 70% sampling ratio

70%	Random	Gaussian	Fourier	Hadamard
RMSE	0.0695	0.0754	0.0261	0.0463
SSIM	0.3763	0.3667	0.6621	0.4374
PSNR	23.1808	22.5154	31.7650	26.6954
end time	86.8023	99.0488	94.6815	85.0416
mask time	3.2721	5.2158	5.0365	4.7600
recon time	83.3141	93.5826	88.4014	79.4868

Table 4.4 : Circles 60% sampling ratio

60%	Random	Gaussian	Fourier	Hadamard
RMSE	0.0736	0.0761	0.0326	0.0524
SSIM	0.3687	0.3648	0.4876	0.4314
PSNR	22.5966	22.3514	29.6570	25.5146
end time	73.3617	86.3436	72.3666	68.5568
mask time	2.9063	4.1452	3.7395	4.0534
recon time	70.2503	81.9420	67.5874	63.7579

Table 4.5 : Circles 50% sampling ratio

50%	Random	Gaussian	Fourier	Hadamard
RMSE	0.0773	0.0737	0.0341	0.2994
SSIM	0.3637	0.3685	0.4855	0.4574
PSNR	22.1748	22.5338	29.2085	10.4523
end time	69.1546	78.5869	66.2060	49.6865
mask time	2.2530	3.5723	3.0438	3.2106
recon time	66.6971	74.7700	62.1665	45.7592

*Best performance for each category is highlighted



Figure 4.1 : Best reconstructed image for binary circles (Hadamard 90%)

As shown in Table 4.1, the best result from RMSE and SSIM is the Hadamard mask. Although the Fourier mask shows a better PSNR, it is only 0.0236 higher. Thus, it can be concluded that overall, the Hadamard Mask (deterministic) is the best for sampling the Binary Circle image (Figure 3.1) at a 90% sampling ratio. For the rest of the sampling ratios, it can be seen that Fourier Mask shows the best results. This shows that for a simple non-random binary image, a deterministic mask works best.

For all sampling ratio, Random masks exhibit the fastest masking time. On the other hand, other than the 90% sampling ratio case, Hadamard mask shows the fastest time for the reconstruction of the image. Masking time is the time taken for the mask to be applied onto the image one after another, the time to sample the image and

produce an output that represents the sparse signal for that image. Reconstruction time is the time taken for the compressive sensing algorithm to convert back that sparse signal into an image.

4.2.2 Cameraman (Figure 3.2)

Table 4.6 : Cameraman 90% sampling ratio

90%	Random	Gaussian	Fourier	Hadamard
RMSE	0.0911	0.0975	0.0774	0.0814
SSIM	0.9272	0.9244	0.9618	0.9673
PSNR	21.0381	20.4197	22.4304	21.9771
end time	71.9615	72.1654	73.8296	70.5902
mask time	4.1542	5.1994	4.5139	4.3488
recon time	67.5645	66.7187	68.4236	65.6377

Table 4.7 : Cameraman 80% sampling ratio

80%	Random	Gaussian	Fourier	Hadamard
RMSE	0.1088	0.1385	0.0905	0.1254
SSIM	0.9049	0.8836	0.9634	0.9037
PSNR	19.6540	17.5546	21.2441	18.3216
end time	69.8103	68.9475	68.5745	65.0338
mask time	3.4584	4.3960	3.8887	4.3038
recon time	66.1562	64.3487	63.7821	59.8354

Table 4.8 : Cameraman 70% sampling ratio

70%	Random	Gaussian	Fourier	Hadamard
RMSE	0.1331	0.1311	0.0950	0.1086
SSIM	0.8492	0.8527	0.9449	0.8453
PSNR	18.3756	18.3133	21.0133	19.8489
end time	62.5036	62.9775	62.8450	59.2065
mask time	3.0274	3.7532	3.5558	3.3957
recon time	59.2714	59.0078	58.3086	55.2147

Table 4.9 : Cameraman 60% sampling ratio

60%	Random	Gaussian	Fourier	Hadamard
RMSE	0.1551	0.1354	0.1246	0.1507
SSIM	0.8040	0.8088	0.9245	0.7226
PSNR	17.0831	18.1788	19.0434	16.7230
end time	54.9866	56.1666	55.5877	46.5523
mask time	2.7612	3.3259	2.9842	2.9566
recon time	51.9951	52.6471	51.7505	42.9877

Table 4.10 : Cameraman 50% sampling ratio

50%	Random	Gaussian	Fourier	Hadamard
RMSE	0.1842	0.1658	0.1732	0.2066
SSIM	0.7725	0.7687	0.8733	0.5538
PSNR	15.8762	16.7552	16.3296	13.6262
end time	51.5221	51.6720	47.9395	42.5470
mask time	2.2499	2.7225	2.5749	2.4440
recon time	49.0754	48.7482	44.4817	39.4966

* Best performance for each category is highlighted



Figure 4.2 : Best reconstructed image for Cameraman (Fourier 90%)

Based on Table 4.6 to Table 4.10, for all of the sampling ratios, Fourier Mask gives the best results for the sampling of the Cameraman image (Figure 3.2). Although based on Figure 3.2, Cameraman is a humanoid figure that exhibits randomness in detail throughout the image, but as it is shrunk down to 64-by-64 pixel for the single pixel sampling, the random details in the face of the Cameraman are barely noticeable. Instead, as the Cameraman image is shrunk down to 64-by-64 pixel, the main body of the image is the body which looks rectangular and simple (Figure 4.2). Thus, this led to a deterministic mask being advantageous for the sampling of this image.

For all sampling ratios, the Random mask exhibit the fastest masking time. On the other hand, for all sampling ratios, Hadamard Mask shows the fastest time for the reconstruction of the image.

4.2.3 Phone (Figure 3.3)

Table 4.11 : Phone 90% sampling ratio

90%	Random	Gaussian	Fourier	Hadamard
RMSE	0.0440	0.0405	0.0379	0.0396
SSIM	0.9278	0.9286	0.9388	0.9343
PSNR	27.0369	27.8909	28.4473	28.0858
end time	95.2952	95.9867	98.5494	96.4459
mask time	28.2004	29.1992	28.2343	28.2069
recon time	66.8102	66.5524	69.3582	67.6079

Table 4.12 : Phone 80% sampling ratio

80%	Random	Gaussian	Fourier	Hadamard
RMSE	0.0444	0.0445	0.0377	0.0450
SSIM	0.9163	0.9201	0.9365	0.9009
PSNR	27.1227	27.1695	28.6539	27.0770
end time	92.9342	93.8433	90.5389	84.3458
mask time	25.2261	26.2185	25.6103	25.1805
recon time	67.4763	67.3939	64.0429	58.5296

Table 4.13 : Phone 70% sampling ratio

70%	Random	Gaussian	Fourier	Hadamard
RMSE	0.0508	0.0527	0.0499	0.0547
SSIM	0.898033	0.8944	0.9124	0.869
PSNR	26.11357	25.83227	26.4525	25.472
end time	83.94627	84.10107	82.1272	76.4744
mask time	22.0593	22.86273	21.9487	22.4094
recon time	61.6509	61.00887	59.2696	53.4008

Table 4.14 : Phone 60% sampling ratio

60%	Random	Gaussian	Fourier	Hadamard
RMSE	0.0540	0.0541	0.0632	0.0653
SSIM	0.8787	0.8818	0.8819	0.8389
PSNR	25.7069	25.6591	24.6348	24.1561
end time	72.9118	73.3669	70.5763	64.6016
mask time	18.8720	19.5312	19.4322	18.8754
recon time	53.7969	53.6054	50.2326	45.0926

Table 4.15 : Phone 50% sampling ratio

50%	Random	Gaussian	Fourier	Hadamard
RMSE	0.0621	0.0620	0.0667	0.1031
SSIM	0.8613	0.8606	0.8822	0.7174
PSNR	24.7004	24.7583	24.5762	19.7228
end time	68.0002	69.0188	62.9051	57.9934

mask time	15.7663	16.5264	15.7263	16.0771
recon time	51.9512	52.2601	46.1850	41.2758

* Best performance for each category is highlighted



Figure 4.3 : Best reconstructed image for Phone (Fourier 90%)

The Phone (Figure 3.3) is a simple rectangular image. Thus, based on earlier inferences, simple non-random images will be led to a deterministic mask being the better mask to sample these images. As shown in Table 4.11 to 4.13, Fourier Mask gives the best results for the sampling of the Phone image. However, as the sampling ratio reduces to 60% and 50%, it could be seen that the pseudo-random mask does provide a better result. The reason is that as pseudo-random masks are generated randomly each time, we need to run and collect the results several times for each sampling ratio. Once the results are collected, the average value is obtained. During this research, 3 runs are done for each sampling ratio for the pseudo-random masks. There might be some runs that the randomly generated masks conform to the image nicely and provide a better result. Thus, at the lower sampling ratios where the deterministic masks aren't sampling the image fully, a random sampling of the image might provide a better result once several runs of sampling are done.

However, the advantage of deterministic masks is that only one run is needed to obtain an accurate result. Every single run with the deterministic mask will provide the same result as the previous run. Thus, this eliminates the randomness during data collection.

For all sampling ratios except 80% sampling ratio, Random masks exhibit the fastest masking time. On the other hand, other than the 90% sampling ratio case, Hadamard mask shows the fastest time for the reconstruction of the image.

4.2.4 Flames (Figure 3.4)

Table 4.16 : Flames 90% sampling ratio

90%	Random	Gaussian	Fourier	Hadamard
RMSE	0.0534	0.0588	0.0706	0.0652
SSIM	0.8604	0.8338	0.7979	0.8631
PSNR	25.4535	24.6263	22.9990	23.8078
end time	111.4153	121.5506	96.4389	93.0554
mask time	26.5824	32.0046	23.7689	23.5407
recon time	84.5887	89.1916	71.7752	68.8690

Table 4.17 : Flames 80% sampling ratio

80%	Random	Gaussian	Fourier	Hadamard
RMSE	0.0454	0.0439	0.0667	0.0603
SSIM	0.8537	0.8551	0.8159	0.8522
PSNR	26.9874	27.3102	23.4840	24.5557
end time	84.3690	84.2194	87.8790	85.6382
mask time	22.1372	21.9989	21.2360	21.2380
recon time	61.9941	61.9880	65.7570	63.5839

Table 4.18 : Flames 70% sampling ratio

70%	Random	Gaussian	Fourier	Hadamard
RMSE	0.0498	0.0497	0.0581	0.0724
SSIM	0.8305	0.8353	0.8502	0.7886
PSNR	26.2342	26.3160	24.7208	22.8297
end time	80.4787	78.6327	80.1150	76.4033
mask time	20.3981	18.7636	18.9263	18.2429
recon time	59.8438	59.6360	59.8006	57.5199

Table 4.19 : Flames 60% sampling ratio

60%	Random	Gaussian	Fourier	Hadamard
RMSE	0.0570	0.0517	0.0615	0.0880
SSIM	0.8006	0.8087	0.8261	0.7112
PSNR	24.9954	25.9308	24.1911	21.1110
end time	86.2266	69.4016	67.8132	87.0140
mask time	21.9365	17.8334	15.7383	28.4180
recon time	64.0572	51.3345	51.1374	57.6824

Table 4.20 : Flames 50% sampling ratio

50%	Random	Gaussian	Fourier	Hadamard
RMSE	0.0754	0.0605	0.0584	0.1492
SSIM	0.7480	0.7626	0.8372	0.5722

PSNR	22.4943	24.0764	24.6525	15.7702
end time	58.8029	59.9543	59.2909	53.9536
mask time	12.6133	13.4539	13.1493	13.5651
recon time	45.9585	46.2676	45.2581	39.7067

*Best performance for each category is highlighted



Figure 4.4 : Best reconstructed image for Flames (Random 90%)

The Flames image (Figure3.4) is a random image, where the details of the image are random and spread throughout the image. Flames can come in many different shapes and forms, thus random. Based on Table 4.16, it can be seen that sampling with the Random mask gives the best result in both the RMSE and PSNR category. Although the Hadamard mask gives a better SSIM result, it is only 0.0029 higher. Thus, it can be shown that the Random mask is the best to sample the Flames image. For the rest of the sampling ratio other than 50% sampling ratio, the Gaussian mask exhibits the best results. Pseudo-random masks are better to sample random images as not only the masks are generated randomly without fixing it, as we need to run the pseudo-random masks several times, some runs are bound to generate a mask that conforms to the random image better.

For all sampling ratios except 50% sampling ratio, Fourier masks exhibit the fastest masking time. Although the Fourier Mask shows the fastest masking time for this image, it is only slightly ahead of the pseudo-random mask. On the other hand, for all of the sampling ratio, the Hadamard mask shows the fastest time for the reconstruction of the image.

4.2.5 Rice (Figure 3.5)

Table 4.21 : Rice 90% sampling ratio

90%	Random	Gaussian	Fourier	Hadamard
RMSE	0.0738	0.0767	0.0855	0.0784
SSIM	0.9260	0.9180	0.8864	0.9284
PSNR	22.0456	21.8675	20.6998	21.9174
end time	73.7094	74.0571	78.5739	73.1531
mask time	4.3221	5.5252	4.6120	4.6372
recon time	68.8300	68.3257	73.0655	67.9394

Table 4.22 : Rice 80% sampling ratio

80%	Random	Gaussian	Fourier	Hadamard
RMSE	0.0825	0.0815	0.0804	0.0792
SSIM	0.9234	0.9176	0.8890	0.9134
PSNR	21.6800	21.7158	20.7417	22.0202
end time	66.4609	65.4362	69.4970	67.9482
mask time	3.9218	4.4278	4.0833	4.0509
recon time	62.2157	60.7953	64.5476	63.3221

Table 4.23 : Rice 70% sampling ratio

70%	Random	Gaussian	Fourier	Hadamard
RMSE	0.0810	0.0836	0.0808	0.0970
SSIM	0.9168	0.9129	0.8809	0.8753
PSNR	22.0374	21.7087	20.5755	21.0927
end time	61.8923	64.4193	63.2501	62.3000
mask time	3.3939	4.1078	3.5735	4.0615
recon time	58.2915	60.1095	58.8400	57.4803

Table 4.24 : Rice 60% sampling ratio

60%	Random	Gaussian	Fourier	Hadamard
RMSE	0.0867	0.0896	0.0882	0.1232
SSIM	0.8953	0.8989	0.8821	0.7902
PSNR	22.0211	21.8793	20.6114	19.3530
end time	53.6234	53.6094	54.2106	48.8590
mask time	2.7145	3.3170	3.0703	2.9817
recon time	50.6705	50.0881	50.2967	45.3188

Table 4.25 : Rice 50% sampling ratio

50%	Random	Gaussian	Fourier	Hadamard
RMSE	0.1095	0.0906	0.0838	0.1121
SSIM	0.8583	0.8483	0.8951	0.6642
PSNR	20.7762	21.4321	21.7444	19.0031
end time	48.1570	49.1200	52.5940	42.4597

mask time	2.3340	2.9215	2.6725	2.5260
recon time	45.6067	45.9768	49.0693	39.3464

*Best performance for each category is highlighted



Figure 4.5 : Best reconstructed image for Rice (Random 90%)

The Rice image (Figure 3.5) is also a random image, with the image showing rice scattering about on a surface. It is included to confirm that pseudo-random masks are better at sampling random images. As shown in Table 4.21, the Random mask gives the best result in the RMSE and PSNR category, with Hadamard Mask showing an SSIM of 0.0024 higher than the random mask. Thus, it can be concluded that the Random Mask is the best for the sampling of the Rice image. For the rest of the sampling ratios except 50% sampling ratio, Random Masks gives the best results.

Although it is shown that pseudo-random masks are better at sampling random images than deterministic masks, it is true only if the deterministic masks are not specially customized to sample a certain image. Based on a paper named “Hadamard single pixel imaging vs Fourier single pixel image” (Zhang, Wang and Zhong, 2016), they found out that by customizing the deterministic masks to the image in question (e.g. a human face), it reconstructs it better than a normal deterministic mask. However, that custom mask can only be used to sample that type of image and will not work well for another random image.

For all sampling ratios, Random masks exhibit the fastest masking time. On the other hand, other than the 80% sampling ratio case, Hadamard mask shows the fastest time for the reconstruction of the image.

4.2.6 Face (Figure 3.6)

Table 4.26 : Face 90% sampling ratio

90%	Random	Gaussian	Fourier	Hadamard
RMSE	0.0600	0.0603	0.0708	0.0706
SSIM	0.7090	0.7084	0.6681	0.6781
PSNR	24.3718	24.2921	22.8878	22.9960
end time	82.5407	81.2877	81.8394	75.4486
mask time	14.6534	15.0529	14.6786	14.7505
recon time	67.6524	66.0276	66.2886	60.0890

Table 4.27 : Face 80% sampling ratio

80%	Random	Gaussian	Fourier	Hadamard
RMSE	0.0543	0.0509	0.0698	0.0759
SSIM	0.7285	0.7348	0.6757	0.6545
PSNR	25.3013	25.8196	23.0219	22.2967
end time	75.7689	80.8684	71.2612	69.0062
mask time	12.8564	13.6694	13.4863	13.7545
recon time	62.6816	66.9455	56.8291	54.4871

Table 4.28 : Face 70% sampling ratio

70%	Random	Gaussian	Fourier	Hadamard
RMSE	0.0534	0.0546	0.0675	0.0742
SSIM	0.7411	0.7433	0.6830	0.6316
PSNR	25.4163	25.3572	23.4291	22.4168
end time	82.4879	90.7483	65.7167	62.2803
mask time	13.9664	16.3298	11.4777	11.6067
recon time	68.2769	74.1533	53.2638	50.0554

Table 4.29 : Face 60% sampling ratio

60%	Random	Gaussian	Fourier	Hadamard
RMSE	0.0549	0.0510	0.0676	0.0750
SSIM	0.7406	0.7548	0.6841	0.5976
PSNR	25.2785	25.8520	23.4471	22.0591
end time	77.2404	61.7865	56.5918	52.9195
mask time	12.7655	10.7907	9.8151	10.1875
recon time	64.2030	50.7895	45.9166	42.1179

Table 4.30 : Face 50% sampling ratio

50%	Random	Gaussian	Fourier	Hadamard
RMSE	0.0506	0.0476	0.0641	0.1114
SSIM	0.7628	0.7702	0.6892	0.5049
PSNR	25.7757	26.2738	23.8227	18.8284
end time	66.8925	54.0815	48.5238	44.6330
mask time	10.4342	8.7499	8.1679	8.3109
recon time	56.1969	45.1122	39.4985	35.5570

* Best performance for each category is highlighted

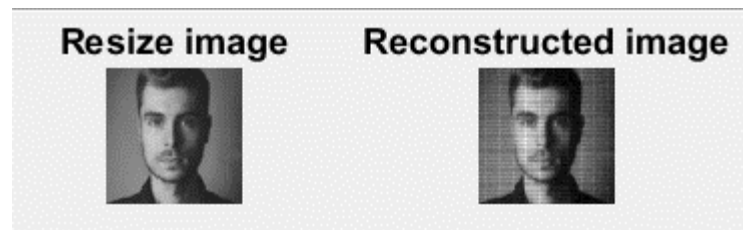


Figure 4.6 : Best reconstructed image for Face (Random 90%)

Face (Figure 3.6) is a random image as all faces are different. There is a different colour, different size and different features for all faces. Based on Table 4.26, Random Mask gives the best results for the sampling of the Face image. For the rest of the sampling ratios, Gaussian Mask gives the best result for sampling the Face image. Both masks are pseudo-random masks.

For sampling ratios 80% and 90%, Random masks exhibit the fastest masking time, with the rest of the sampling ratios showing Fourier Masks having a slightly faster masking time. On the other hand, for all of the sampling ratios, the Hadamard mask shows the fastest time for the reconstruction of the image.

4.2.7 FUW chart (Figure 3.7)

Table 4.31 : FUW chart 90% sampling ratio

90%	Random	Gaussian	Fourier	Hadamard
RMSE	0.0474	0.0448	0.0295	0.1519
SSIM	0.613	0.6252	0.7679	0.4312
PSNR	26.5515	27.0484	30.7421	16.3727
end time	100.2495	100.0509	103.1744	95.0633

mask time	21.54427	22.0243	21.3662	21.8368
recon time	77.77263	77.8090	80.9289	72.6488

Table 4.32 : FUW chart 80% sampling ratio

80%	Random	Gaussian	Fourier	Hadamard
RMSE	0.0656	0.0600	0.0730	0.2468
SSIM	0.5575	0.5718	0.5388	0.3332
PSNR	23.5472	24.3482	22.6084	12.1298
end time	87.4066	90.2140	88.9944	92.8839
mask time	18.6319	19.3962	19.3049	21.7099
recon time	68.5270	70.6052	68.8931	70.6039

Table 4.33 : FUW chart 70% sampling ratio

70%	Random	Gaussian	Fourier	Hadamard
RMSE	0.0880	0.0937	0.0862	0.1877
SSIM	0.5165	0.5021	0.512	0.3556
PSNR	21.3558	20.5894	21.0506	14.6101
end time	78.4977	79.9306	85.2271	74.6694
mask time	16.4700	17.1164	17.0728	16.7979
recon time	61.8087	62.5998	67.2779	57.3107

Table 4.34 : FUW chart 60% sampling ratio

60%	Random	Gaussian	Fourier	Hadamard
RMSE	0.0994	0.1203	0.1267	0.2426
SSIM	0.4896	0.4551	0.4475	0.3085
PSNR	20.0238	18.3775	18.0056	12.1305
end time	68.9271	69.8880	69.1194	71.9040
mask time	14.1497	14.6375	14.7220	15.2180
recon time	54.5614	55.0326	53.5637	56.1151

Table 4.35 : FUW chart 50% sampling ratio

50%	Random	Gaussian	Fourier	Hadamard
RMSE	0.1517	0.1362	0.1498	0.1702
SSIM	0.4070	0.4245	0.3972	0.4601
PSNR	16.4982	17.3407	16.4462	15.1176
end time	63.0186	63.7937	60.1467	55.0679
mask time	11.8573	12.4248	12.5316	12.0140
recon time	50.9510	51.0691	46.7899	42.3932

* Best performance for each category is highlighted

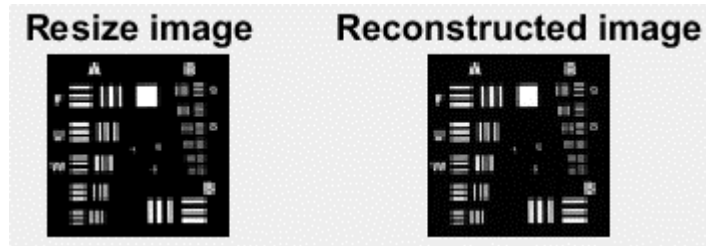


Figure 4.7 : Best reconstructed image for FUW chart (Fourier 90%)

As shown from Table 4.31, Fourier Mask gives the best results for the sampling of the FUW chart (Figure 3.7). The FUW image is an image where there are a series of lines in both vertical and horizontal directions, together with alphabets in different sizes. Many researches use this image to test their image reconstruction methods, thus this image is added for a comparison to other research. Although the Fourier mask shows the best results at a 90% sampling ratio, once the sampling ratio drops to 70% and below, it seems that the pseudo-random masks are showing better results. This could be due to the intricate details on the FUW chart. As the sampling ratio for the deterministic masks lowers, it is harder to sample all the small details on the masks, thus leading to the pseudo-random masks showing better results.

For all sampling ratios except 90% sampling ratio, Random masks exhibit the fastest masking time. On the other hand, other than the 80% and 70% sampling ratio case, Hadamard mask shows the fastest time for the reconstruction of the image.

4.2.8 Hadamard 50% Sampling Error

During the data collection for this research topic, a peculiar error was encountered. As sampling ratios for the Hadamard mask drops to 50% and lower, there seems to be an error in sampling and reconstructing the image.

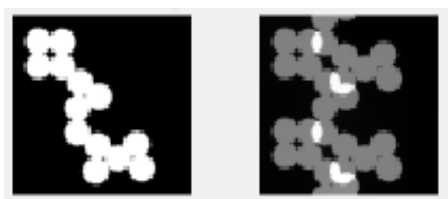


Figure 4.8 : Binary Circles 50% Hadamard Mask Sampling Error

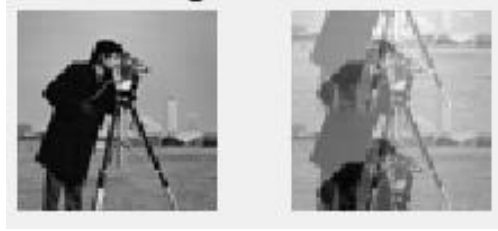


Figure 4.9 : Grayscale Cameraman 50% Hadamard Mask Sampling Error

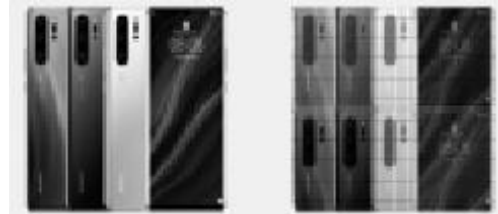


Figure 4.10 : Phones 50% Hadamard Mask Sampling Error

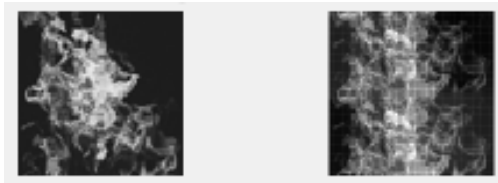


Figure 4.11 : Flames 50% Hadamard Mask Sampling Error



Figure 4.12 : Rice 50% Hadamard Mask Sampling Error

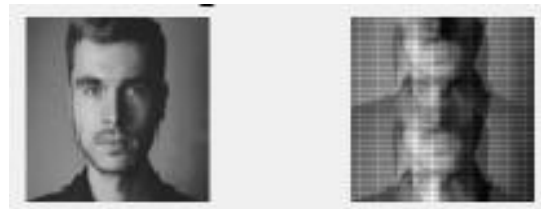


Figure 4.13 : Face 50% Hadamard Mask Sampling Error



Figure 4.14 : FUW Chart 50% Hadamard Mask Sampling Error

As shown from Figure 4.8 to 4.14, the reconstructed image from a 50% sampling ratio of Hadamard mask seems to show overlapping of image. Sampling ratio under 50% for Hadamard mask too exhibit this problem. However, for the rest of the masks, there seems to be no such problem.

This error most likely arises from coding issues during simulation of single pixel imaging, as other research doesn't seem to have this issue when the sampling ratio is below 50%.

4.3 Summary of Result Analysis

In terms of mask time, the Random mask is more efficient, consistently shows the shortest mask time regardless of the sampling ratio. Meanwhile, for Gaussian/Fourier/Hadamard, mask time increases with the sampling ratio.

The Random mask uses uniform distribution function, masks with 0 and 1 are generated easily with the MATLAB function as it is built-in without any need for modification. For the Gaussian Mask case, masks are generated with values ranging from negative to positive. Therefore, there is an extra step in changing values that are negative to 0 and positive to 1 to create a mask, thus extra masking time. Fourier and Hadamard are the same, which is creating a complete mask, in the beginning, using their respective function, and then reconstructing it every iteration of sampling by making adjustments to the original masks. Therefore, their masking time is almost the same. All 4 masks' masking time increase with the sampling ratio. Mask time is drastically different for different images.

Masks for Random/Gaussian is different every time a mask is generated. Therefore, an averaging method must be done to the results as there are masks that provide a nice result and vice versa. This is a disadvantage as overall, to get an accurate

result, several runs are needed. On the other hand, Fourier/Hadamard Masks will get the same RMSE, PNSR, and SSIM every single time as they are the same masks, there is no random element in generating and masking the image. Therefore, not only that it is possible to pre-generate and pre-load the mask, but it is also faster because we do not need to sample the image more than 1 time to get an accurate result.

In terms of reconstruction time, all 4 patterns consistently increase with a higher sampling ratio. Overall, Fourier/Hadamard has lower reconstruction time. There are several explanations for this. Other than 2 exceptions, Hadamard has the fastest reconstruction time for all sampling ratios across all images. First, as Random/Gaussian Masks needs to be averaged after 3 samplings, this means that there could be long and short reconstruction time in between those 3 runs. This will lead to an average result, but not as accurate as deterministic masks. Second, as we transpose the Hadamard matrix to reconstruct the mask, it is inherently faster compared to other masks (based on an earlier literature review), thus making Hadamard mask the mainstream mask for single pixel imaging. Circles, Phone, FUW chart, Cameraman* images are considered the same type of object, simple objects that are round/square-ish. Both of these images have a better result with deterministic masks. (* With cameraman resized down to 64-by-64 pixel, the body of the image is simple and squarer looking as the random features of the face is barely visible) Circles, phone, etc, the way the details are structured in the image is similar to the masks. The circles in the Circles image are in positions that are similar to the Hadamard mask, thus making the mask ideal to sample the image.

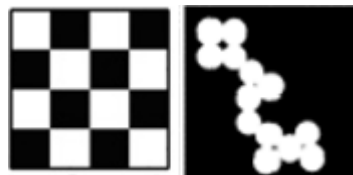


Figure 4.15: Visual example of how a mask conforms to an image

Random/Gaussian masks will perform better in images that are random in nature such as Face, Flames and Rice images as the masking patterns are random, and that the results are from averaging 3 runs. Thus, among those runs, there might be a mask that conforms to the image better and give a better result. However, if the Hadamard/Fourier masks are patterned in such a way that it conforms to the image that

we are sampling (flames/face), it will produce a better result than Random/Gaussian masks. The Fourier vs Hadamard paper (Zhang, Wang and Zhong, 2016) has several examples that as they change the Hadamard/Fourier pattern from square to diamond, it performs better on human faces. In the paper, it states that Fourier is better, but with tweaks to Hadamard mask the way it samples the images (diamond, zigzag, square, spiral, etc), Hadamard will provide a faster and better-quality image.

Table 4.36 : Advantages vs Disadvantages of Pseudo-random Masks

Advantage	Disadvantage
Universal (doesn't need to know the image beforehand)	Unable to reproduce results consistently
Better for random looking image (rice, face, flames, etc)	Unable to pre-load and pre-generate the mask

Table 4.37 : Advantages vs Disadvantages of Deterministic Masks

Advantage	Disadvantage
Results is able to be reproduced consistently	Have to know the image beforehand and create a custom mask to better sample the image
Able to pre-generate and pre-load the mask	
Better quality image if masks is suitable to sample the image	

CHAPTER 5

CONCLUSION AND RECOMMENDATION

5.1 Conclusion

Single pixel imaging is an-emerging method that could change how we sample images in the future. However, as single pixel imaging technique is still in the early stages of development, extensive research is needed before it can become an effective alternative to conventional imaging methods such as CCD or CMOS. This project aims to analyse different light modulation and sampling methods as well as their influence on the single pixel imaging.,

Based on the data analysis, Random Mask has the fastest masking time overall, while Hadamard Mask has the shortest reconstruction time. In term of image quality, Pseudo-random Masks give better RMSE, PSNR, and SSIM for random looking images such as Face, Flames and Rice. On the other hand, Deterministic masks show better results for non-random images such as Circles, Phones, and humanoid figures.

Although there are many advantages to apply Pseudo-random masks such as simpler mask construction and no prior knowledge is needed on the image being sampled. Unfortunately, it has a significant disadvantage of not being able to be pre-loaded and pre-generated. In practice, this is important as masks that can be pre-loaded and pre-generated can save a huge amount of time especially if the sampling needs to be done in real-time such as a CCTV camera. Even though Deterministic masks aren't as good in sampling random-looking images but this can be further improved with certain customization. If we are to know the type of image that we are sampling beforehand, such as a face detection only CCTV, we can create a custom Deterministic mask that especially conforms to the shape of a face, which greatly increasing its accuracy. In addition, Deterministic masks do not need to sample the image several times to get an accurate result as the consistency of the results is guaranteed.

In conclusion, Deterministic masks are better than Pseudo-random masks generally., However, there are advantages of Pseudo-random masks that might make it more suitable in some circumstances. The findings established in this project are important to provide a comprehensive understanding of various mask patterns, their characteristics and impacts to the application of single pixel imaging.

5.2 Limitations

There are a few limitations during this research. First of all, the maximum size of the image that could undergo this single pixel imaging simulation is only 64-by-64 pixels. Images that are larger than this needs to be shrunk down to 64-by-64 pixels. Thus, this limits the data collection on finer details on a larger image that could affect the results inferred.

In addition, there was some errors in the Hadamard mask sampling once the sampling ratio reduces to 50% and below. This limits the research as we are unable to compare the image that is sampled below 50% sampling ratio. Lastly, as single pixel imaging currently only works in grayscale, we are unable to obtain data on the reconstruction of colour images.

5.3 Recommendation for Future Research

Further research can be considered by identifying and correcting the error in Hadamard mask sampling for 50% and lower sampling ratio. This allows the research to be extended on lower sampling ratios for simpler images. This could be possible by collaborating with other existing research that managed to sample below 50% sampling ratio.

Besides, the research can be expanded to sample and reconstruct colour images, as currently colour images are not possible to be sampled and reconstructed for single pixel imaging. Furthermore, explore other potential application which allow it to be a strong contender for conventional imaging methods that are more expensive and bulkier.

REFERENCES

- Aksenov, M. D. and Sych, D. V. 2018 ‘Optimal Data Acquisition Methods for Single-Pixel Imaging’, *Journal of Russian Laser Research*, 39(5), pp. 492–498.
- Al-Kheer, Abd Al-Kareem. (2010). Integrating the concepts of optimization and reliability in the design of agricultural machines.
- Augustin, S. *et al.* 2018 ‘Mask responses for single-pixel terahertz imaging’, *Scientific Reports*, 8(1), pp. 1–7.
- Barnett, S. M. *et al.* 2017 ‘Adaptive foveated single-pixel imaging with dynamic supersampling’, *Science Advances*, 3(4), p. e1601782.
- Brown, E. A. and Grice, J. W. 2011 ‘One is Enough’, *SAGE Open*, 1(3), p. 215824401142864.
- Bryan, K. and Leise, T. 2013 ‘Making Do with Less: An Introduction to Compressed Sensing’, *SIAM Review*, 55(3), pp. 547–566.
- Cand, E. J. 2008 ‘The restricted isometry property and its implications for compressed sensing’, *Comptes Rendus Mathematique*, 346(9–10), pp. 589–592.
- Candès, E. J., Romberg, J. K. and Tao, T. 2006 ‘Stable signal recovery from incomplete and inaccurate measurements’, *Communications on Pure and Applied Mathematics*, 59(8), pp. 1207–1223.
- Chen, J. 2019 *Normal Distribution: Definition*, 7 may. Available at: <https://www.investopedia.com/terms/n/normaldistribution.asp> (Accessed: 24 February 2020).
- Deng, L. 2014 ‘Uniform Distribution: Definitions and Properties’, *Wiley StatsRef: Statistics Reference Online*, pp. 1–3.
- Edgar, M. P., Gibson, G. M. and Padgett, M. J. 2019 ‘Principles and prospects for single-pixel imaging’, *Nature Photonics*, 13(1), pp. 13–20.
- Hadamard, J. 1893 ‘Resolution of a question on determinants’.
- How to Calculate Root Mean Square Error (RMSE) in Excel - GIS Geography* 2014. Available at: <https://gisgeography.com/root-mean-square-error-rmse-gis/> (Accessed: 24 February 2020).
- Lustig, M., Donoho, D. and Pauly, J. M. 2007 ‘Sparse MRI: The application of compressed sensing for rapid MR imaging’, *Magnetic Resonance in Medicine*, 58(6), pp. 1182–1195.

Mitra, K., Cossairt, O. and Veeraraghavan, A. 2014 ‘Can we beat Hadamard multiplexing? Data driven design and analysis for computational imaging systems’, *2014 IEEE International Conference on Computational Photography, ICCP 2014*. IEEE, pp. 1–9.

Nguyen, T. L. N. and Shin, Y. 2013 ‘Deterministic Sensing Matrices in Compressive Sensing: A Survey’, *The Scientific World Journal*, 2013(4), pp. 1–6.

Nowak, R. 2006 ‘Compressive Sensing: A New Framework for Imaging’. Available at: www.ece.wisc.edu/~nowak.

Peak Signal-to-Noise Ratio as an Image Quality Metric - National Instruments 2019. Available at: <https://www.ni.com/en-my/innovations/white-papers/11/peak-signal-to-noise-ratio-as-an-image-quality-metric.html> (Accessed: 24 February 2020).

Pierce, Rod. 2019, 'Normal Distribution', Math Is Fun, Available at: <http://www.mathsisfun.com/data/standard-normal-distribution.html>. (Accessed 9 May 2020)

R.Fisher *et al.* 2003 *Image Transforms - Fourier Transform*. Available at: <https://homepages.inf.ed.ac.uk/rbf/HIPR2/fourier.htm> (Accessed: 24 February 2020).

Rousset, F. *et al.* 2017 ‘Adaptive Basis Scan by Wavelet Prediction for Single-Pixel Imaging’, *IEEE Transactions on Computational Imaging*, 3(1), pp. 36–46.

Shannon, C. E. 1998 ‘Communication In The Presence Of Noise (Republished)’, *Proceedings of the IEEE*, 86(2), pp. 447–457.

SSIM: Structural Similarity Index | imatest (no date). Available at: <http://www.imatest.com/docs/ssim/> (Accessed: 24 February 2020).

Sun, M. J. *et al.* 2017 ‘A Russian Dolls ordering of the Hadamard basis for compressive single-pixel imaging’, *Scientific Reports*. Springer US, 7(1), pp. 1–7.

Taylor, S. A. 1998 ‘CCD and CMOS Imaging Array Technologies: Technology Review’, *Xerox Research Centre Europe*, pp. 1–14.

Vasconcelos, N. 2015 *Discrete Cosine Transform*. Available at: <http://www.svcl.ucsd.edu/courses/ece161c/handouts/DCT> (Accessed: 24 February 2020).

Wang, Z. *et al.* 2004 ‘Image quality assessment: From error visibility to structural similarity’, *IEEE Transactions on Image Processing*, 13(4), pp. 600–612.

Wang, Z., Simoncelli, E. P. and Bovik, A. C. 2003 ‘Multi-scale structural similarity for image quality assessment’, *Conference Record of the Asilomar Conference on*

Signals, Systems and Computers, 2(Ki L), pp. 1398–1402.

Yu, W.-K. and Liu, Y.-M. 2019 ‘Single-pixel imaging with origami pattern construction’, pp. 1–12. Available at: <http://arxiv.org/abs/1903.11432>.

Yu, W. K. *et al.* 2014 ‘Complementary compressive imaging for the telescopic system’, *Scientific Reports*, 4, pp. 1–6.

Zhang, Y. 2013 ‘Theory of Compressive Sensing via ℓ_1 -Minimization: A Non-RIP Analysis and Extensions’, *Journal of the Operations Research Society of China*, 1(1), pp. 79–105.

Zhang, Z., Wang, X. and Zhong, J. 2016 ‘Fast Fourier single-pixel imaging using binary illumination’, 37(5), pp. 605–609. Available at: <http://arxiv.org/abs/1612.02880>.

Zhou, C. *et al.* 2018 ‘Multi-resolution Progressive Computational Ghost Imaging’, 2. Available at: <http://arxiv.org/abs/1811.01733>.